



universität  
wien

# MASTERARBEIT / MASTER'S THESIS

Titel der Masterarbeit / Title of the Master's Thesis

**„Detection of pulsed ionising radiation in medical applications“**

verfasst von / submitted by

Reinhard Stefan Wagner, BSc

angestrebter akademischer Grad / in partial fulfilment of the requirements for the degree of

Master of Science (MSc)

Wien, 2021 / Vienna, 2021

Studienkennzahl lt. Studienblatt /  
degree programme code as it appears on  
the student record sheet:

UA 066 876

Studienrichtung lt. Studienblatt /  
degree programme as it appears on  
the student record sheet:

Masterstudium Physik

Betreut von / Supervisor:

Hon.-Prof. Dipl.-Phys. Dr. Eberhard Widmann

# Contents

<b>Acknowledgements</b>	<b>1</b>
<b>Abstract</b>	<b>2</b>
<b>1 Theoretical background</b>	<b>3</b>
1.1 Ionising radiation . . . . .	3
1.2 Interactions of ionising radiation . . . . .	4
1.2.1 Charged particles . . . . .	4
1.2.2 Bremsstrahlung . . . . .	5
1.2.3 Electromagnetic waves . . . . .	6
1.3 Biological effects of ionising radiation . . . . .	7
1.3.1 Deterministic effects . . . . .	7
1.3.2 Stochastic effects . . . . .	8
1.4 Dose values . . . . .	9
1.4.1 Protection quantities . . . . .	9
1.4.2 Operational quantities . . . . .	10
<b>2 Ionising radiation in medical applications</b>	<b>12</b>
2.1 The development of radiology . . . . .	12
2.2 Frequency of ionising radiation applications . . . . .	13
2.3 Austrian legislation . . . . .	14
2.4 X-ray generators . . . . .	15
<b>3 Fluoroscopy</b>	<b>18</b>
<b>4 Measurement devices</b>	<b>21</b>
4.1 Individual monitoring . . . . .	21
4.2 Area monitoring . . . . .	22
4.3 Austrian legislation . . . . .	23
4.4 Detector types . . . . .	23
4.4.1 Ionisation chamber . . . . .	24
4.4.2 Scintillation counter . . . . .	25
4.4.3 Semi conductor . . . . .	26
4.5 Detection of pulsed radiation . . . . .	26
<b>5 Experimental setup</b>	<b>27</b>
5.1 Radiation source . . . . .	27
5.2 Radiation settings . . . . .	28
5.2.1 Examination type . . . . .	28
5.2.2 Radiation mode . . . . .	29
5.2.3 Pulse rate . . . . .	29
5.2.4 Voltage . . . . .	29
5.2.5 Exposure size of image intensifier . . . . .	29
5.2.6 Radiation time . . . . .	29

5.3	Measurement devices . . . . .	30
5.3.1	Szintomat 6134 A/H . . . . .	32
5.3.2	6150AD-b/E . . . . .	32
5.3.3	GammaTwin . . . . .	33
5.3.4	LB 123 Umo . . . . .	33
5.3.5	TOL/F LB 1320 . . . . .	34
5.3.6	6150AD6/E . . . . .	34
5.3.7	EPD Mk2 . . . . .	35
5.3.8	EPD TruDose G . . . . .	35
5.3.9	Rad-60SE . . . . .	36
5.4	Experimental geometry . . . . .	36
5.4.1	Stray radiation . . . . .	36
5.4.2	Useful radiation . . . . .	38
<b>6</b>	<b>Results</b>	<b>39</b>
6.1	Pre-measurements . . . . .	39
6.2	Stray radiation . . . . .	40
6.2.1	$H^*(10)$ devices . . . . .	42
6.2.2	$H_x$ devices . . . . .	43
6.2.3	$H_p(10)$ devices . . . . .	44
6.2.4	Comparison of categories . . . . .	45
6.2.5	Comparison of detector type . . . . .	47
6.2.6	Comparison of all devices . . . . .	48
6.3	Useful radiation . . . . .	49
6.4	Recommendations . . . . .	51
	<b>List of Figures</b>	<b>54</b>
	<b>List of Tables</b>	<b>55</b>
	<b>Bibliography</b>	<b>58</b>
	<b>Glossary</b>	<b>59</b>

# Acknowledgements

This thesis has been written with the professional and personal support of many people. It is important to me to make these contributions visible and to thank them.

First, I want to thank my supervisor Eberhard Widmann for his trust and valuable guidance throughout my studies. His advice was always helpful and there when needed. I hope to stay in contact beyond the timeframe of this thesis.

I also want to point out the invaluable technical expertise of Christoph Stettner, without whose support this thesis would not have been possible.

Last, but not least, I want to thank my family, who let me find my own way in life and encouraged me throughout. In addition, I would like to thank my girlfriend who always had a sympathetic ear, offered good advice, and helped me to rest my mind outside of my research.

Further people who have contributed significantly in different ways to this thesis and whom I would like to thank are: Alexander Stolar, Alfred Hefner, Andreas Steurer, Christian Hranitzky, Christoph Marek, Johannes Neuwirth, Martin Kopecky, Nadine Baumgartner and many more.

A special thanks to Seibersdorf Laboratories for the provision of the necessary equipment and the opportunity to write my master's thesis alongside my regular job.



# Abstract

## English

In contrast to conventional X-ray imaging, where only single images are taken, fluoroscopy enables the observation of dynamic processes. This method is used in a variety of medical examinations and can either be realised via continuous or pulsed ionising radiation. The use of pulsed radiation determines a reduction of dose for the patient but generates challenges for measurement devices. The majority of currently used devices are optimised for the use in continuous radiation fields. Therefore, difficulties can arise when measuring pulsed radiation, which in the worst case can lead to an underestimation of radiation dose. Although papers addressing this issue do exist, quantitative studies have only been done for a small number of devices of which the majority is not used in Austria. This thesis examines devices, which can be officially calibrated in Austria and are therefore in broad use.

The aim of this thesis is to review the function of various measurement devices in the pulsed radiation field of a C-arm. Based on these results recommendations for the operators of such devices are formulated, which shall lead to an improved radiation protection of people working with pulsed ionising radiation in medical applications.

Terms that the reader is not expected to be familiar with are written in italics and explained in the glossary.

## Deutsch

Im Gegensatz zu konventionellen Röntgenaufnahmen, wo nur Einzelbilder aufgenommen werden, ermöglicht Durchleuchtung die Beobachtung von Prozessen. Diese Methode wird bei einer Vielzahl von medizinischen Untersuchungen angewandt und kann sowohl durch kontinuierliche oder gepulste Strahlenexposition realisiert werden. Die Verwendung von gepulster Strahlung führt zu einer Reduktion der Patientendosis, schafft allerdings Probleme für Messgeräte dieser Strahlung. Die meisten der eingesetzten Messgeräte sind für kontinuierliche Strahlenfelder optimiert. Dementsprechend können Probleme bei der Messung von gepulsten Strahlenfeldern auftauchen, was im schlimmsten Fall zu einer Unterschätzung der Strahlendosis führen kann. Obwohl Paper zu diesem Thema existieren beziehen sich bisherige Studien nur auf eine geringe Anzahl an Messgeräten, die nicht in Österreich eingesetzt werden. Diese Arbeit untersucht Messgeräte, die in Österreich eichfähig sind und dementsprechend weitläufig eingesetzt werden.

Das Ziel dieser Arbeit ist die Überprüfung der Funktion verschiedener Messgeräte im gepulsten Strahlungsfeld eines C-Bogens. Basierend auf den Resultaten werden Empfehlungen für die Nutzer dieser Geräte gegeben, was zu einem besseren Strahlenschutz für Personen führen soll, die in gepulsten Strahlenfeldern medizinischer Anwendungen arbeiten.

Begriffe mit denen die Leserin bzw. der Leser vermutlich nicht vertraut ist sind kursiv geschrieben und im Glossar erklärt.

# Chapter 1

## Theoretical background

A deeper understanding of any topic is preceded by a study of the fundamental theoretical background. The aim of this chapter is to prepare the reader for the performed experiments and their relevance. Naturally, the amount of needed explanation depends on the readers prior knowledge. This thesis is aimed at physicists with a background in nuclear and particle physics, wherefore familiarity with these fields is presumed and only important principles are being illustrated. The medical facets of the subject, on the other hand, are explained in more detail.

### 1.1 Ionising radiation

Ionisation is every process where an electrically neutral atom loses electrons, transforming it into an ion. This can be induced by the interaction with particle or electromagnetic radiation, provided the transferred energy exceeds the binding energy of the electron. Therefore, the binding energy of the weakest bound electron is equivalent to the ionisation energy of the atom, making ionisability dependent on the atomic structure. Considering Caesium with the lowest ionisation energy of 3.9 eV, any kind of radiation with an energy of 3.9 eV or more is able to induce ionisation. This theoretical conclusion however is unsuitable for practical applications and especially lawmaking. The Austrian Law for Radiation Protection (LRP) defines ionising radiation follows:

§ 3 (33) Ionising radiation: Energy, which is transferred in form of particles or electromagnetic waves with a wavelength of 100 nm or less (a frequency of  $3 \text{ E}+15$  Hertz or more) and can directly or indirectly produce ions.<sup>1</sup> [1]

This definition is consistent with the definition of the International Commission on Radiation Units and Measurement (ICRU):

"Ionising radiation consists of charged particles or uncharged particles (e.g. photons) capable of causing ionisation by primary or secondary processes." [2, p. 4]

It is noticeable, that the ICRU uses a rather self-explaining definition but refrains from setting a definition in terms of energy.

---

<sup>1</sup>§ 3 (33) Ionisierende Strahlung: Energie, die in Form von Teilchen oder elektromagnetischen Wellen mit einer Wellenlänge von 100 Nanometern oder weniger (einer Frequenz von  $3 \text{ E}+15$  Hertz oder mehr) übertragen wird, die direkt oder indirekt Ionen erzeugen können.

This can be attributed to the dependence of ionisation energy on the specific material and evaluated process. In order to set a norm for the estimation of radiation dose, the International Commission on Radiological Protection (ICRP) defined a reference body [3]. On the condition that an element has to make up at least 1 g of the 70 kg reference body, the model consists of 15 elements [3, p. 327-328]. The quantity-weighted mean ionisation energy of these 15 elements is 12,9 eV which corresponds to a wavelength of 96 nm [4, p. 930]. This similarity suggests, that the model serves as a template for the legal definition of the LRP. It should be noted, that even if present in public discourse, non-ionising radiation is not part of radiation protection which solely engages with the protection of humans and the environment from the dangers of ionising radiation. If not explicitly noted, the term radiation in this thesis always refers to ionising radiation.

## 1.2 Interactions of ionising radiation

Prerequisite for the effects of ionising radiation is interaction, the type of which depends on the interacting material and the radiation itself. In this chapter only radiation types and energy levels relevant for medical diagnostics and X-ray generators are covered.

### 1.2.1 Charged particles

Charged particles interact via the Coulomb force with the absorbing material. The type of interaction primarily depends on the impact parameter  $s$  which is the distance between the trajectory of the incoming particle and the barycentre of the interaction. [5, p. 248-249]. This is illustrated in figure 1.2.1:

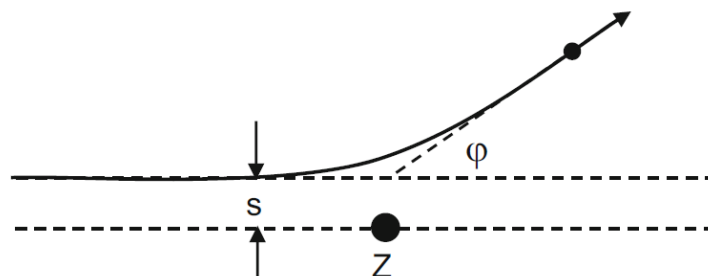


Figure 1.2.1: Definition of the impact parameter  $s$  with impact centre  $Z$  and scattering angle  $\varphi$ . [5, p. 248]

Based on the proportion of impact parameter  $s$  and atom size  $r_{\text{atom}}$  a classification of the Coulomb interaction can be made:

#### Big impact factor ( $s \gg r_{\text{atom}}$ )

In the event of big impact factor the particle interacts with the entire electron shell. This can lead to the deformation and polarisation of the electron shell, resulting in a small energy loss and change of flight path of the incoming particle due to momentum conservation (elastic scattering). If an outer electron gets excited or ionised the incoming particle loses the excitation, respectively ionisation energy and changes its flight path (inelastic scattering).

Due to the small ionisation energy of the electrons in the outer atomic shell the ionised electrons lose their energy fast and deposit it locally. Both processes, inelastic as well as elastic scattering induce the transfer of small energy amounts, which constitute up to 50% of the total energy loss. [5, p. 249] Due to the various small energy transfers the incoming particle loses its energy continuously.

### Medium impact factor ( $s \approx r_{\text{atom}}$ )

With impact factors on the scale of the atomic radius, interactions with single shell electrons take place. Thereby, the energy transfer is much higher and the ionised electrons ( $\delta$ -electrons) are able to ionise further atoms themselves. Due to the bigger energy transfer these interaction are also called hard collisions.

### Small impact factor ( $s \ll r_{\text{atom}}$ )

If the energy of the incoming particle is high enough to transit the electron shell it can directly interact with the nucleus. Although the possibility for an scattering without energy loss does exist, these events are rare. Standard is the scattering in the Coulomb field of the nucleus, accompanied by the emission of electromagnetic radiation (Bremsstrahlung).

## 1.2.2 Bremsstrahlung

Bremsstrahlung is the foundation of X-ray generation. The radiation intensity depends on the deflection angle, which is directly proportional to the energy of the incoming particle and indirectly to  $s$ . The dependence of the radiant braking capacity  $S_{\text{rad}}$  for a particle of charge ( $z \cdot e$ ) and mass  $m$  in the Coulomb field of a nucleus can be approximated as follows: [5, p. 264-265]

$$S_{\text{rad}} = \left( \frac{dE}{dx} \right)_{\text{rad}} \propto \rho \cdot \left( \frac{ze}{m} \right)^2 \cdot \frac{Z^2}{A} \cdot E_{\text{tot}} \quad (1.1)$$

The directional distribution of the emitted photons depends on the energy of the incoming particle and thickness of the target. For thin absorbers there is a distinct angular distribution, in thick absorbers, multiple interactions result in a more isotropic distribution. The angular distribution with electrons as incoming particles is shown in figure 1.2.2: [5, p. 267,268]

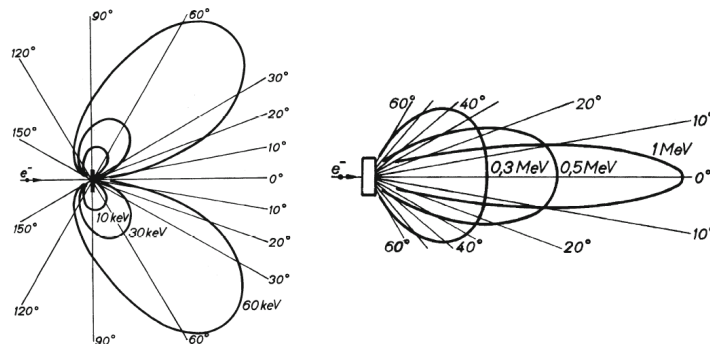


Figure 1.2.2: Angular photon distribution for thin absorbers (left) and thick absorbers (right). [5, p. 268]

### 1.2.3 Electromagnetic waves

The interactions of electromagnetic waves are characterised by less frequent but intense occurrences. The importance of the basic interactions photo effect, Compton effect and pair production depend on the energy of the incoming photon and the atomic number  $Z$  of the interaction partner, which is illustrated in figure 1.2.3:

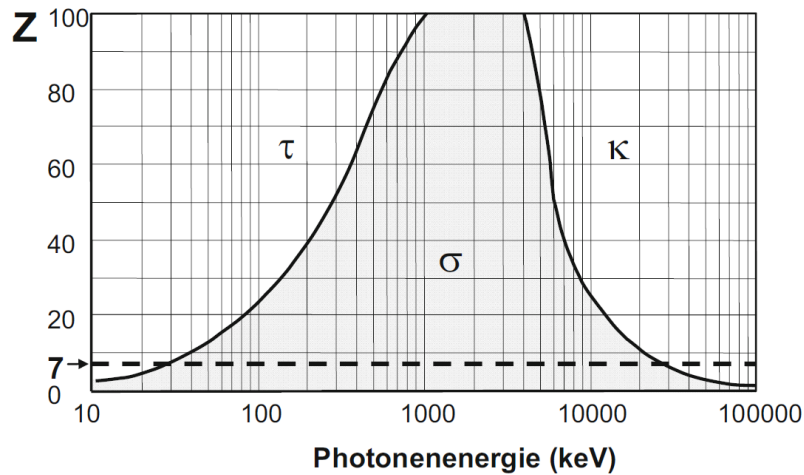


Figure 1.2.3: Areas representing the dominance of photo effect  $\tau$ , Compton effect  $\sigma$  and pair production  $\kappa$ . The dotted line at  $Z = 7$  represents the medium atomic number of human tissue and phantom materials. [5, p. 193]

At X-ray energies for medical diagnosis ( $\approx 100$  keV) and human tissue ( $Z \approx 7$ ) the Compton scattering is the dominant interaction. This has to be considered for X-ray imaging as well as radiation protection. Lead aprons ( $Z = 82$ ) on the other hand work due to the photo effect.

The Compton effect describes the inelastic scattering of a photon on a weakly bound electron in one of the outer shells of the atom. Energy and momentum are distributed depending on the scattering angle with a maximum at  $180^\circ$ . The Compton interaction coefficient  $\sigma_C$  is proportional to the ratio between proton number  $Z$  and mass number  $A$ . Important in terms of radiation protection, especially for scattered radiation in medical applications, is the dependence of scattering angle from photon energy. This, based on the Klein-Nishina formula, is shown in Figure 1.2.4:

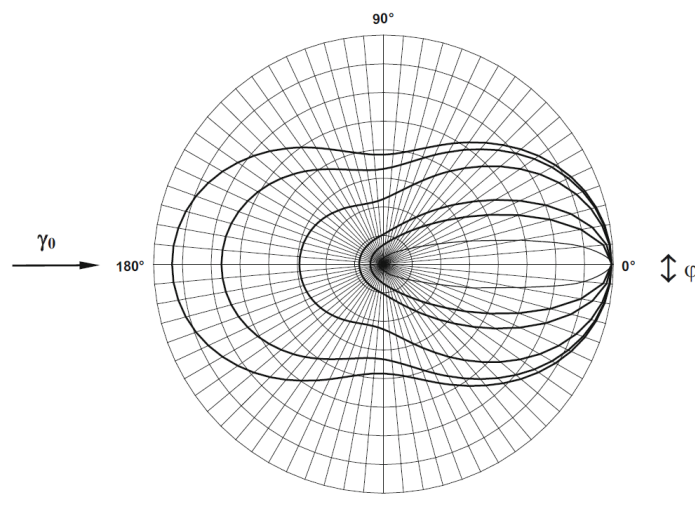


Figure 1.2.4: Photon energy dependence on the scattering angles. From left to right: 10, 50, 200 keV, 1, 2 and 10 MeV. [5, p. 171]

## 1.3 Biological effects of ionising radiation

With physics being a descriptive science, the ionisation process does not carry any value in terms of being positive or negative. However, when considering the effects of this process on living cells, it can either have a positive or a negative effect. Positive and negative are hereby characterised by either an increase or decrease in the chance of survival. Despite the theoretical possibility of an evolutionary advantage by a cell change due to an ionisation process, the disadvantageous cell changes clearly dominate. Therefore the exposure to ionising radiation is considered harmful, making it desirable to limit radiation exposure for the individual, as well as to society.

If ionising radiation interacts with an atom of a biological cell, the initial physical interaction induces a chemical and biological reaction. The type of biological response by the cell depends on the properties of the radiation, as well as the type of cell itself. The *radiosensitivity* of a cell is directly proportional to the cell division rate and inversely proportional to the degree of *cell differentiation* [6, p. 179]. This can be attributed to the shorter correction response time at high cell division rates, as well as the compensability of damaged cells at low development stages. Especially the first factor highlights the importance of radiation protection for human embryos, where severe malformations can occur with doses above 0.25 Sv [6, p. 179].

### 1.3.1 Deterministic effects

The exposure to high levels of ionising radiation causes to the formation of acute effects. These so called deterministic effects occur due to the *necrosis* of multiple cells and the accompanying inability to perform their task. In return this means, that deterministic effects only emerge at sufficient numbers of cell deaths, thus setting a dose limit. *Somatic reactions* to ionising radiation are observable in the *haemogram* after the exposure to an effective dose higher than 250 mSv [6, p. 179], which corresponds to more than 55 times the average annual radiation exposure of the Austrian population (4.5 mSv) [7, p. 7]. The correlation between radiation dose and severeness of the radiation damage is shown in figure 1.3.1:

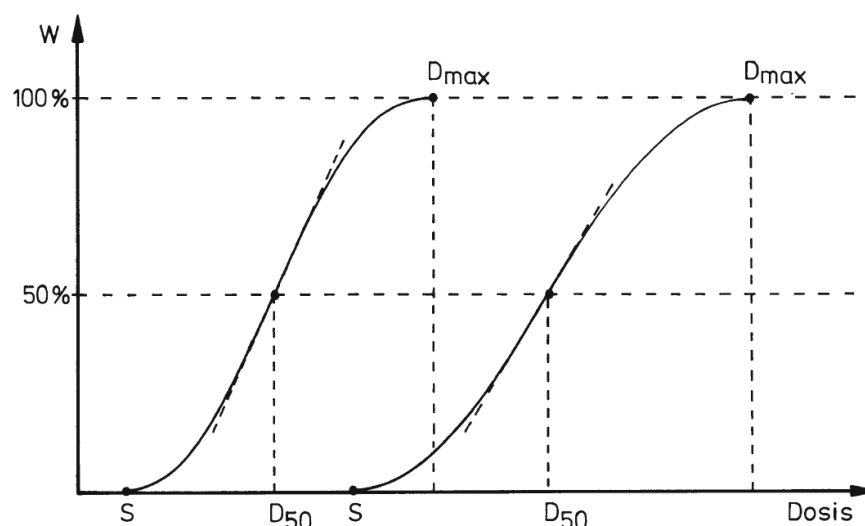


Figure 1.3.1: Typical sigmoidal curve shape for the relative effect function of deterministic effects. Individual curves vary in terms of dose threshold  $S$ , slope, 50%-dose  $D_{50}$ , saturation dose  $D_{max}$  and depend both on the irradiated tissue as well as the type of ionising radiation. [5, p. 437]

In this context severeness of radiation damage not only refers to the scale of clinical symptoms like *radiation erythema* or the *acute radiation syndrome*, commonly known as radiation sickness, but also on the *latency period* until the first symptoms appear. After the exposure to a radiation dose above the threshold, symptoms inevitably appear, hence the characterisation as deterministic effects. However, it should be noted that although still commonly used, the term "deterministic effects" is controversial. The ICRP declares in its paper "Statement on Tissue Reactions":

"[...] These effects, previously called deterministic effects, are now referred to as tissue reactions because it is increasingly recognised that some of these effects are not determined solely at the time of irradiation but can be modified after radiation exposure." [8, p. 1]

In medical diagnostic single imaging, tissue reactions are generally not relevant. However, in fluoroscopy, tissue reactions, in form of radiation erythema, have been observed [9].

### 1.3.2 Stochastic effects

Stochastic effects have no threshold and emerge due to DNA-changes. These changes can either appear due to direct ionisation, especially *DNA double strand breaks*, as well as by *radicals*, generated by the ionisation of water molecules. In contrast to tissue reactions, the received dose does not determine the severeness of a radiation damage, but the probability of its occurrence. Correlation functions are based on the *Life Span Study* (LSS), a research program investigating lifelong health effects of atomic bomb survivors. The findings of this epidemiological study suggest a linear relation between dose and damage probability. In their 2007 recommendation, the ICRP quantifies the additional risk for fatality, due to excessive cancer and heritable effect, at 5% per Sievert. [10, p.12]. Health effects of small doses of radiation ( $< 100$  mSv per year) are currently under discussion. Possible relations are shown in figure 1.3.2:

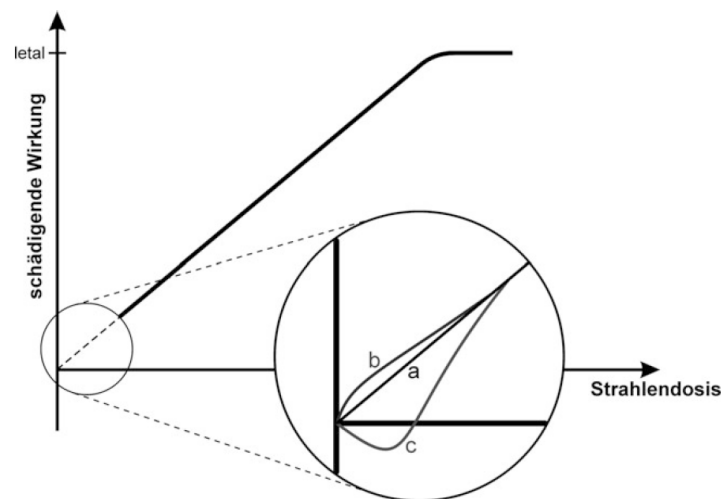


Figure 1.3.2: Possible relations of dose and radiation damage. [11, p. 91]

The *Linear No Threshold* (LNT) model (a) is currently recommended by the ICRP [10, p. 43]. The overreaction at small doses (b) is reasonable under the assumption, that repair mechanisms only become operative at threshold impairments. While some studies suggest an positive health effect of small radiation doses, also known as hormesis (c), due to the conservative principle of radiation protection this model is highly disputed.

The main problem in the task of clarifying health effects of small radiation doses is the signal to noise ratio. With currently one in five people worldwide being diagnosed with cancer in their lifetime [12, p. 13], the excess risk of 0.5% for 100 mSv would require an enormous amount of participants for epidemiological studies in order to get statistically significant results. A task group of the ICRP states:

"However, the problem of quantifying risks that are so low as to be practically unobservable, and then recommending policies based on that quantification, is very difficult. It is highly likely that there will always be uncertainty about the risk of low doses, and that we will have to come to terms with that uncertainty." [13, p. 39]

Nevertheless, ensuing a conservative safety first mindset, radiation protections attempts to prevent unnecessary and minimise inevitable radiation exposures.

## 1.4 Dose values

Due to the damaging effect of ionising radiation even at low doses it is important to measure and interpret levels of radiation exposure in terms of their hazard potential. The scientific pursuit of measuring radiation dose and dose rate is called dosimetry and requires two types of quantities:

**Protection quantities:** used to relate radiation dose to radiation risk

**Operational quantities:** used to assess the protection quantities in terms of measurement

The so called absorbed dose  $D$  is used as the basic physical quantity. It is defined as the quotient of the mean energy  $d\bar{\epsilon}$  transferred to matter of mass  $dm$  [10, p. 62]:

$$D = \frac{d\bar{\epsilon}}{dm} \quad (1.2)$$

Instead of the SI unit  $\text{J kg}^{-1}$  the Unit Gray (Gy) is used. The absorbed dose enables to quantify radiation fields. However, it does not predict the potential harm by the specific exposure.

### 1.4.1 Protection quantities

The equivalent dose  $H_T$  of an organ or tissue T additionally considers the hazard potential of a radiation R with the radiation weighting factor  $w_R$ :

$$H_T = \sum_R w_R D_R \quad (1.3)$$

Despite  $w_R$  being a dimensionless factor, in order to clarify the demarcation from the sole physical quantity  $D$ , the unit Sievert (Sv) is used. This distinction is important for the estimation of stochastic damage, because the exposure to 1 mGy of alpha radiation ( $w_R=20$ ) has 20 times the potential of inducing stochastic effects than the exposure to 1 mGy of gamma radiation ( $w_R = 1$ ). The values of  $w_R$  are based on experimental data of the *Relative Biological Effectiveness* (RBE).



The second important factor, when considering the probability of stochastic effects, is the radiation sensitivity of different tissue. The effective dose  $E$  takes this into account with the tissue weighting factor  $w_T$ :

$$E = \sum_T w_T H_T = \sum_T w_T \sum_R w_R D_R \quad (1.4)$$

The unit of  $E$  is also Sievert (Sv). The values for  $w_T$  are derived from epidemiological studies and enable the calculation of the risk for stochastic effects, even for partial exposures. For example, the danger for the induction of stochastic effects due to a full body exposure of 1 mSv is the same as for a 25 mSv exposure of the thyroid gland ( $w_T = 0.04$ ).

Additionally to the dose, the respective dose rates can be defined, which is the measured radiation dose per time interval. Common units are  $\mu\text{Sv/h}$  and  $\text{mSv/h}$ .

## 1.4.2 Operational quantities

Although the protection quantities are used to specify exposure limits to ensure that the occurrence of stochastic health effects is kept below unacceptable levels [10, p. 63], they are not directly measurable. Therefore, operational quantities, serving as a conservative estimate of the protection quantities, are defined. [10, p. 71] Hereby it is important to be aware of different radiation qualities and penetration depths, which is why a further distinction is made between operational quantities for individual- and area monitoring.

### Individual monitoring

Operational quantities for individual monitoring, represented by  $H_p(d)$ , enable the measurement of the equivalent dose in the soft tissue at a representative part of the body [5, p. 318]. The parameter  $d$  defines the depth of measurement in the soft tissue in mm. For deep penetrating radiation  $H_p(10)$  is used. It serves as an estimate for the effective or organ dose. For low penetrating radiation  $H_p(0.07)$  is used. It serves as an estimate for the skin dose at the point, where the dosimeter is worn. It is also used in ring dosimeters, for the estimation of the dose for the hands.

Further standards are in discussion, as stated by the ICRP:

"A depth of  $d=3$  mm has been proposed for the rare case of monitoring the dose to the lens of the eye. In practice, however,  $H_p(3)$  has rarely been monitored and  $H_p(0.07)$  can be used for the same monitoring purpose." [10, p. 71]

It has to be noted, that the measured dose in individual monitoring is also dependent on the carrier of the dosimeter. Due to the influence of stray radiation and absorption in the carrier, the measured dose can vary from person to person, even if they are exposed to the same radiation field.

## Area monitoring

All quantities for area monitoring are defined on the basis of a dose equivalent at a point in a simple phantom, the ICRU sphere. [10, p. 297]. For deep penetrating radiation, the ambient dose equivalent  $H^*(d)$  is used with the assumption, that the incoming direction of arrival is not important (signified by the \*). The parameter  $d$  defines the depth of measurement in the ICRU sphere in mm. Usually  $H^*(10)$  is used.

For low penetrating radiation the incoming direction matters, therefore the directional dose equivalent  $H'(d, \Omega)$  is used. Hereby  $\Omega$  is the direction vector of the incoming radiation. Exemplary is the use of  $H'(0.07, \Omega)$ .

Both quantities are distinct from the general equivalent dose in empty space due to the measuring depth and the consideration of stray radiation. The disregard of back scattered radiation can distort the measurement by up to 50% [5, p. 315-318]

Another operational quantity is the photon equivalent dose  $H_x$ . It was introduced in Germany in the 1980s but recognised internationally. However, there are still measurement devices that can be officially calibrated in Austria, that measure the photon equivalent dose.

Besides the previously explained quantities of  $H_p(10)$ ,  $H^*(10)$  and  $H_x$ , the air kerma, as explained in chapter 3, is also relevant. In order to compare these quantities, conversion factors are needed. However, due to the variety of dependencies like radiation geometry and energy dependence, any comparison of quantities in a real, not idealised radiation field must be understood as a rough approximation. For example, the conversion factors assume idealised radiation fields. The application on a whole, real X-ray spectrum therefore automatically distort the result.

# Chapter 2

## Ionising radiation in medical applications

Ionising radiation is used in medicine in three ways [14]. Diagnostic radiology uses X-ray generators to obtain images of the inside of a patient's body. Nuclear medicine uses radioactive substances, introduced into the patient, for diagnosis or treatment. Radiotherapy uses many types and sources of ionising radiation, to cure or relieve symptoms of cancer and other diseases. In this thesis the term "radiology" is used synonymous with "diagnostic radiology".

### 2.1 The development of radiology

The discovery of X-rays in November 1895, and the inventions resting upon it, revolutionised medical diagnostics. Contrary to many other groundbreaking inventions, an application for the newly found X-rays by Wilhelm Conrad Roentgen was clear from day one [15, p. 357-360]. Although Roentgen could not have foreseen today's application of X-ray in medical diagnoses and therapy, he laid the foundation by refusing to patent his discovery with the goal to let it be adapted for practical needs by various companies [16, p. 50-51]. In the year 1896 fluoroscopy, which enabled the observation of continuous processes within the body, was developed. [17, Das konventionelle Röntgen bis 1900] Hereby, the afterglow of fluorescent screens or plates, coated with special phosphorus compounds, was used, the method of use is shown in figure 2.1.1:

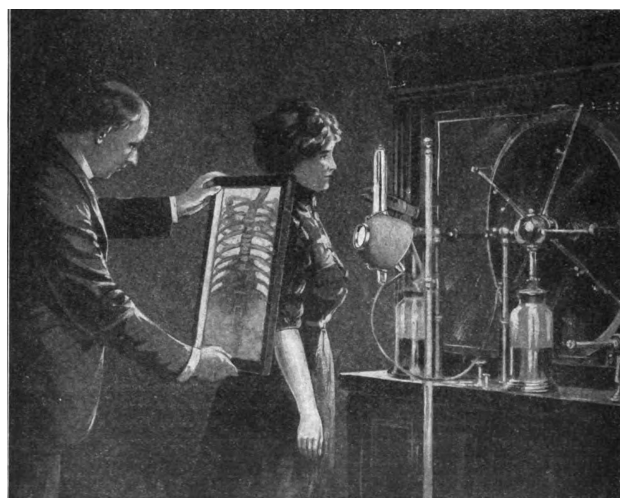


Figure 2.1.1: Early application of fluoroscopy. The useful beam is directed on the patient and radiologist who observes the X-ray projection on a fluorescent plate. No precautions for radiological protection were taken. [18, p. 6]

Despite first stories about radiation damages being reported already in March 1896 due to long exposure times of up to one hour, the cases increased drastically in 1904. Clarence M. Dally, assistant of Thomas A. Edison, died from the consequences of radiation exposure and numerous radiologist experienced damages on their left hands, which they used to adapt the depth of focus of the fluoroscope. [17, Das konventionelle Röntgen von 1901 - 1950] Still, first basic approaches for radiation protection by dentist William H. Rollins got no attention. Instead the subsequent decades yielded capital developments in the field of *interventional radiology* and *sectional imaging techniques*, like computer tomography (CT), which made *exploratory surgery* mostly obsolete. [11, p. 122]

Nowadays the possibilities of conventional radiology have largely been explored [17, Entwicklung der Röntgentechnik]. The current focus for conventional radiology is on digitising imaging and optimising radiation protection. Sectional imaging techniques, however, are on the rise.

## 2.2 Frequency of ionising radiation applications

In modern medicine, the application of ionising radiation is standard procedure and frequently used. In Austria, 1468 examinations per 1000 inhabitants are conducted in the field of radiology per year, including interventions (status 2015) [19, p. 7]. Here, one must bare in mind, that the frequency of a certain procedure and the radiation dose caused by it, do not necessarily correlate, as can be seen in figure 2.2.1:

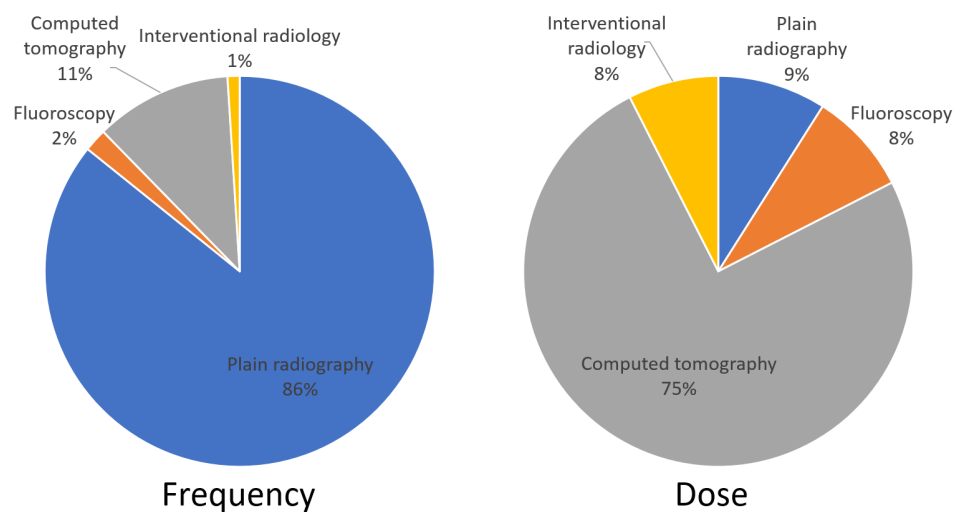


Figure 2.2.1: Frequency of various examination methods using ionising radiation and the share of the collective dose caused by it. [19, p. 8]

Despite being categorised separately, many radiological interventions use fluoroscopy. With this in mind the use of fluoroscopy, which accounts for under 2.9% of all examination methods using ionising radiation, is responsible for 8.5-16% of the collective dose. Overall the use of ionising radiation in medical procedures with 1.7 mSv/year accounts for the biggest share of the 4.5 mSv/year average annual radiation exposure of the Austrian population [7, p. 7]. However, one must bear in mind that this value is an average distorted by applications with low frequency but high dose (e.g. CT).

## 2.3 Austrian legislation

The use of ionising radiation in medical applications in Austria is regulated by one law and two administrative orders:

- Law for Radiation Protection 2020 (Strahlenschutzgesetz 2020)
- General Radiation Protection Ordinance 2020 (Allgemeine Strahlenschutzverordnung 2020)
- Medical Radiation Protection Ordinance (Medizinische Strahlenschutzverordnung)

The fundamental criterion for the authorisation of any application of ionising radiation in Austria is § 4 of the Law for Radiation Protection:

**§ 4 (1)** New activities may only be authorised or permitted, if they are justified in the sense, that it can be reasonably assumed, that the benefits to the individual or to society, associated with the activity, outweigh the harm to health, that may be caused by the exposure.<sup>1</sup> [1]

The Medical Radiation Protection Ordinance (MRPO) specifies this in § 3 for medical applications, by requiring an upfront justification of every single examination and, where appropriate, the consideration of available previous images. The consideration of necessity of a radiation application is up to the doctor, whereby methods with comparable knowledge gain but less radiation exposure have to be taken into account. Since every application of ionising radiation increases the risk for stochastic damages, an unjustified application is considered as personal injury under the Austrian law. Another cornerstone of radiation protection is optimisation, which is regulated in § 5 of the LRP:

**§ 5 (1)** Radiation protection of persons subject to public or occupational exposure shall be optimised with the aim of keeping the level of individual doses, the probability of exposure and the number of persons exposed, as low as reasonably achievable, taking into account the current state of technical knowledge, as well as economic and social factors.<sup>2</sup> [1]

Optimisation not only determines a continuous technical development, but also the use of the hereby gained knowledge for radiation protection. It is based on the LNT model by assuming that even small radiation doses increase the risk of stochastic effects. While the risk of small exposures for the individual might be negligible, when considering the entire population even small risks result in observable cases.

Both justification and optimisation are specifications of the informal "As Low As Reasonably Achievable (ALARA)" principle, which can be seen as the paradigm of radiation protection.

---

<sup>1</sup>§ 4 (1) Neue Tätigkeiten dürfen nur bewilligt oder zugelassen werden, wenn sie insofern gerechtfertigt sind, als dass begründet angenommen werden kann, dass der mit der Tätigkeit verbundene Nutzen für die Einzelne/den Einzelnen oder für die Gesellschaft die durch die mit der Tätigkeit verbundenen Exposition möglicherweise verursachte gesundheitliche Schädigung überwiegt.

<sup>2</sup>§ 5 (1) Der Strahlenschutz von Personen, die der Exposition der Bevölkerung oder einer beruflichen Exposition ausgesetzt sind, ist mit dem Ziel zu optimieren, die Höhe der Individualdosen, die Wahrscheinlichkeit einer Exposition sowie die Anzahl der exponierten Personen unter Berücksichtigung des jeweils aktuellen technischen Erkenntnisstandes sowie wirtschaftlicher und gesellschaftlicher Faktoren so niedrig wie vernünftigerweise erreichbar zu halten.

## 2.4 X-ray generators

The Law for Radiation Protection defines a radiation generator as follows:

§ 3 (69) Radiation generator: a radiation source capable of producing ionising radiation such as X-rays, neutrons, electrons or other charged particles, where the radiation does not emanate from radioactive substances.<sup>3</sup> [1]

If the emitted radiation is X-rays, one can speak of X-ray generators. These generators form the basis of the majority of medical devices, that use ionising radiation for diagnostic imaging. Despite the prodigious scientific and technical progress of recent times, current tubes have not changed significantly since 1900 [20, p. 5-1]. This is particularly evident in the low efficiency, with only 1% of the energy being converted into radiation. [11, p. 126]. The production of X-rays is based on the interactions described in section 1.2.1. In an X-ray tube, a filament is heated by a heating voltage and emits electrons. These are accelerated by an acceleration voltage  $U_a$  between cathode and anode, which for medical diagnostics usually is between 30-150 kV [11, p. 125]. When they hit the anode material X-rays are generated as well as heat.

The structure of an X-ray tube with its main components is shown in figure 2.4.1:

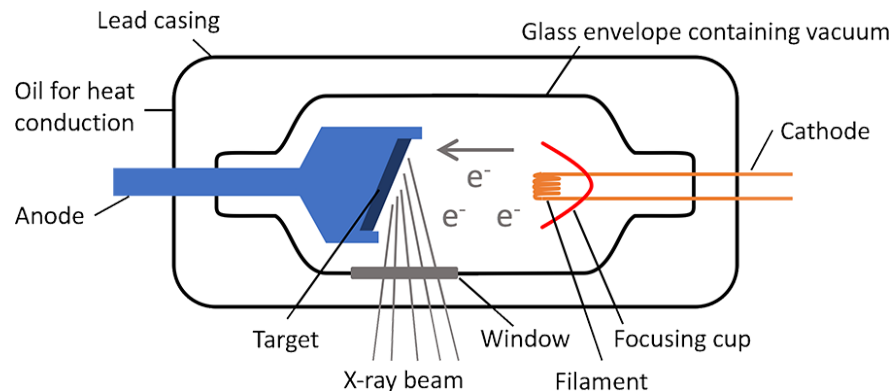


Figure 2.4.1: Schematic structure of an X-ray tube. [21, p. 8]

The main components are:

**Casing:** Within the glass envelope there is vacuum, which shall ensure that the only interaction of electrons is with the anode material. The lead casing shields stray radiation from the anode. Oil is used for heat dissipation between the glass envelope and lead casing.

**Tube window:** Used to limit the size of the useful X-ray beam.

**Filament:** Is heated and emits electrons for acceleration.

**Cathode (Focusing cup):** Focuses the accelerated electrons on a focal point on the anode target. The size of the focal point has an important impact on image quality.

**Anode (Target):** Gets hit by the accelerated electrons and emits X-rays due to interactions on the atomic level. Due to the high heat production, various techniques, like rotation of the anode, are used to prevent overheating.

<sup>3</sup>§ 3 (69) Strahlengenerator: eine Strahlenquelle, die ionisierende Strahlung wie Röntgenstrahlung, Neutronen, Elektronen oder andere geladene Teilchen erzeugen kann, wobei die Strahlung nicht von radioaktiven Stoffen ausgeht.

The emitted photons are not mono-energetic but form a spectrum. A schematic energy spectrum, typical for medical X-ray generators, is shown in figure 2.4.2:

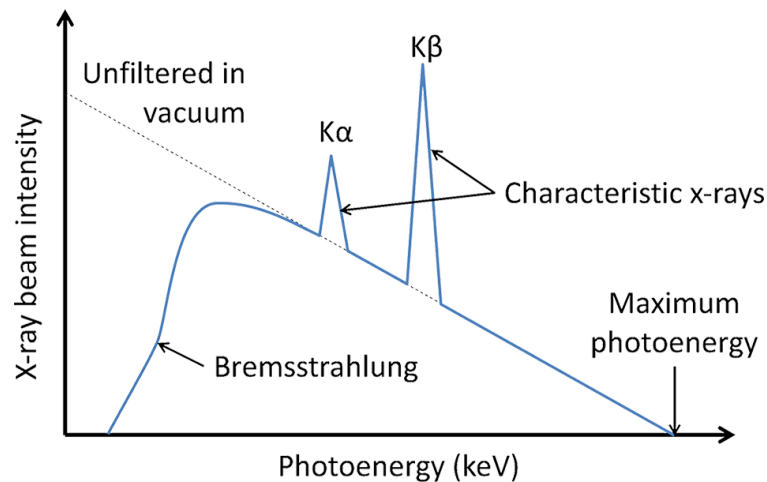


Figure 2.4.2: Typical X-ray spectrum. [22, Production of X-ray]

The depicted spectrum is the sum of two separate spectra, the spectrum of the Bremsstrahlung and the characteristic X-rays.

Bremsstrahlung already appears at low energies. The maximum photon energy  $E_{\gamma, \max}$  can be calculated as follows:

$$E_{\gamma, \max} = e \cdot U_a = h \cdot \frac{c}{\lambda_{\min}} \quad (2.1)$$

The dependence of the photon energy on the continuous impact factor  $s$  described in chapter 1.2.1 results in a continuous spectrum of the Bremsstrahlung. This is illustrated in figure 2.4.2 by the line labeled with "Unfiltered in vacuum". However, in reality the effect of filtration has to be taken into account. When a spectrum of photons interacts with matter, low energy photons are over-proportionally absorbed. This causes a lack of low energy photons in the X-ray spectrum. Low energy photons cause a radiation dose for the patient but can not be used for imaging. Therefore additional filters (e.g. aluminium) are used to harden the energy spectrum.

If the accelerated electrons have enough energy to ionise atoms in the anode material, one obtains characteristic X-rays, which depend on the specific atoms of the anode material. Some medical examinations, like mammography, primarily use these characteristic X-rays for imaging.

The main parameters influencing the X-ray spectrum are voltage, current and filtration. In figure 2.4.3 effects on the X-ray spectrum, by the variation of these parameters, are illustrated:

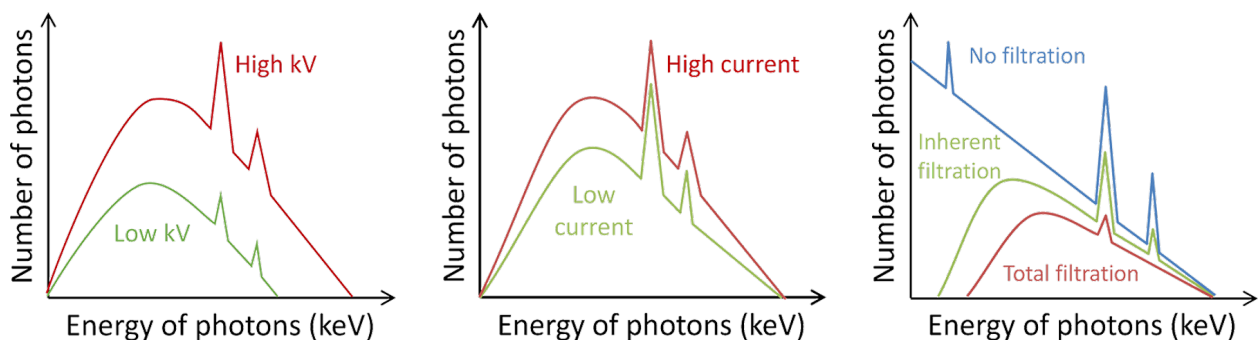


Figure 2.4.3: Effect on the spectrum by voltage (left), current (middle) and filtration (right). [22, Production of X-ray]

The effects on the X-ray spectrum by the individual parameters are as follows:

**Voltage:** Higher voltage increases the amount of X-ray photons, the average energy and the maximum energy. If the voltage is high enough, depending on the anode material, characteristic lines can appear in the spectrum. The maximum photon energy, also labeled as nominal voltage, has a fundamental effect on the penetration power of the X-rays.

**Current:** Increases the quantity of photons with all other characteristics being unaffected.

**Filtration:** Increases the average energy of photons while decreasing the total number of photons.

An X-ray tube in use produces various radiation fields as shown in figure 2.4.4:

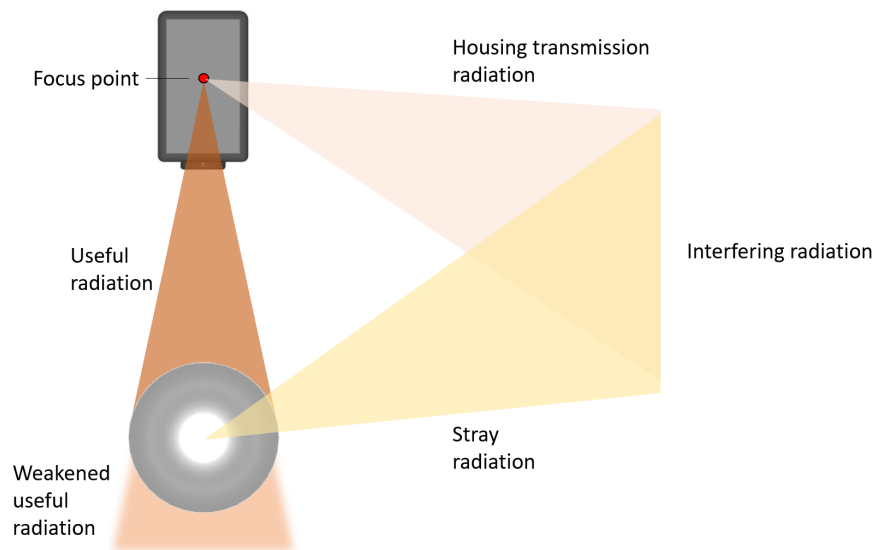


Figure 2.4.4: Radiation fields of the an X-Ray tube.

The part of the radiation emitted by the X-ray tube that is used for imaging is called useful radiation. Another relevant field in terms of radiation protection is stray radiation, which are diverted photons of the useful radiation. Together with the housing transmission radiation it is called interfering radiation. X-ray tubes in medical applications with a nominal voltage under 150 kV, must have a housing tube radiation dose of less than 1 mSv/h in 1 m distance. [23, p. 12]



# Chapter 3

## Fluoroscopy

Fluoroscopy is used for real-time observation in the body by imaging techniques based on ionising radiation. Possible procedures are versatile and range from simple positioning of bones or implants to complex procedures in *interventional radiology*. In contrast to single radiographic shots, the radiation parameters, especially tube current, are reduced. However, with longer exposition times, the dose for the patient can exceed the one of single shots considerably, which is why the MRPO sets measures for the dose reduction in fluoroscopy:

**§ 27 (3)** Facilities for fluoroscopy must be equipped with automatic dose rate control and an X-ray image intensifier or equivalent devices.<sup>1</sup> [24]

An automatic dose rate control compares requested and measured detector output and adapts peak tube voltage and tube current to provide an optimal image for different patients and examinations. However, care must be taken not to insert high density objects, such as radiation protection gloves, into the radiation path. This would cause the automatic dose regulation system to increase the radiation parameters, causing additional dose for the patient.

An X-ray image intensifier uses a photocathode and photomultiplier to intensify the image produced by the system and make it available for the display on a screen. This drastically reduces the dose necessary for a diagnosable image compared to traditional fluorescent screens.

Further regulations for the use of fluoroscopy are set in § 28 of the MRPO:

**§ 28 (3)** In surgical and interventional radiology procedures, dose saving procedures and equipment such as pulsed radiation and image storage must always be used.<sup>2</sup> [24]

Image storage keeps the last taken image on the screen, which is especially important for interventional radiology, where breaks for further planning of the procedure are necessary.

Pulsed radiation saves radiation dose, by emitting multiple short radiation pulses instead of a constant one.

---

<sup>1</sup>§ 27 (3) Einrichtungen für Durchleuchtungen müssen mit einer automatischen Dosisregelung und einem Röntgenbildverstärker oder einer gleichwertigen Vorrichtung ausgestattet sein.

<sup>2</sup>§ 28 (3) Bei chirurgischen und interventionsradiologischen Eingriffen sind grundsätzlich dosissparende Verfahren und Einrichtungen wie gepulste Strahlung und Bildspeicher zu verwenden.

The process of fluoroscopy can be divided into two steps, the production and the detection of X-rays. Both components can be either be continuous or pulsed.

Only the use of traditional fluorescent screens allows an continuous observation of the detected X-rays. In modern methods like image intensifiers or solid state detectors the display on the screen is pulsed, even if due to the high frame rates of modern screens the human eye perceives it as a continuous image.

More important however is the production of X-rays, which can either happen continuously or pulsed, which is defined as follows:

"A continuous radiation field for the application in area and individual dosimetry is an ionising radiation field with a constant dose rate at a given point for periods longer than 10 s, if the power on and off processes are neglected. A pulsed radiation field for the application in area and individual dosimetry is an ionising radiation field which is not a continuous radiation field." [25, p. 484]

For the characterisation of fluoroscopy in pulsed or continuous only the type of production of the X-rays is relevant.

Figure 3.0.1 illustrates the difference in dose of pulsed and continuous radiation:

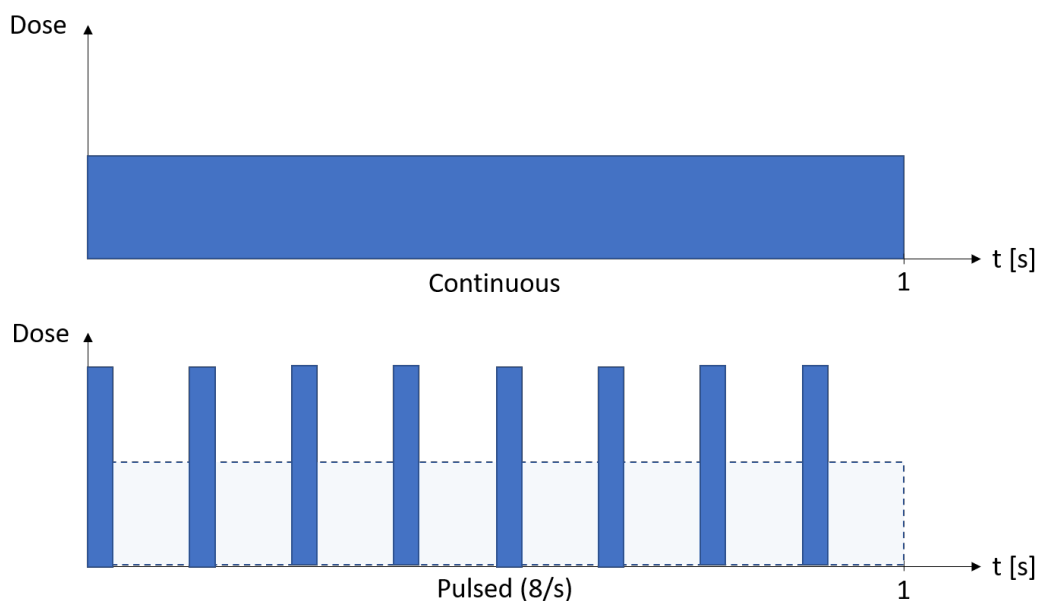


Figure 3.0.1: Schematic plot of the radiation dose of continuous and pulsed fluoroscopy

Pulsed fluoroscopy is characterised by short, intense radiation pulses. This combination of short radiation duration and very high dose rate can cause problems in the detection, especially if the measurement devices are optimised for continuous radiation fields. [26, p. 1]

In figure 3.0.2 the parameters characterising a radiation pulse are visualised:

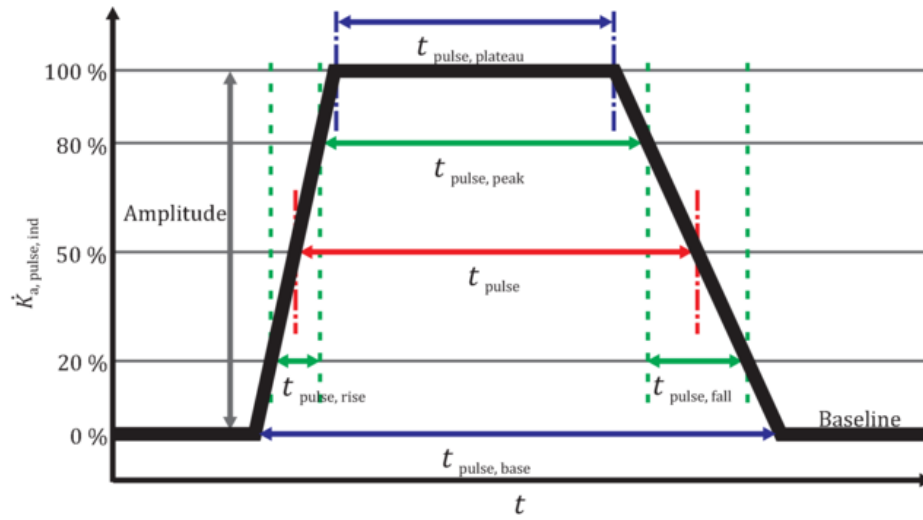


Figure 3.0.2: Equivalent trapezoidal radiation pulse with the relevant parameters. [27, p. 5]

The indicated air kerma pulse rate  $\dot{K}_{a,pulse,ind}$  which is given in the y-axis is the quotient of the air kerma per radiation pulse and the radiation pulse duration. [27, p. 4] The kinetic energy released per mass (Kerma) is an important measurement parameter in detector physics and indicates the sum of initial kinetic energies of all charged particles liberated by uncharged ionising radiation. [28]

Of all possible parameters used to characterise a radiation pulse the main are:

- Pulse duration [s]:  $t_{pulse}$
- Pulse dose rate [Sv/s]:  $\dot{H}_{pulse}$
- Pulse frequency [Hz]:  $f_{pulse}$
- Pulse dose [Sv]:  $H_{pulse}$

The pulse dose rate can easily be calculated by the following relation:

$$\dot{H}_{pulse} = \frac{H_{pulse}}{t_{pulse}} \quad (3.1)$$

For medical X-ray facilities the pulse duration ranges from 10 s to 1 ms. The dose rate in the pulse in 1 m distance from the focal point is up to 40 mSv/s. The maximum dose rate of continuous X-ray facilities is 1.5 mSv/s in 1 m distance from the focal point. [29]

# Chapter 4

## Measurement devices

As shown in section 1.4, the quantification of radiation fields is important for the estimation of potential harm for the individual or society. In this thesis, a special focus is laid on measurement devices for individual and area monitoring of radiation fields produced by medical devices used for diagnostics.

### 4.1 Individual monitoring

Individuals exposed to ionising radiation in the course of their professional practice are subject to special legal provisions. The LRP defines radiation exposed workers as follows:

**§ 3 (68)** Radiation exposed worker: a person who is exposed in the course of its work and who is likely to receive radiation doses exceeding one of the dose limits established for public exposure [1 mSv].<sup>1</sup> [1]

The General Radiation Protection Ordinance (GRPO) further subdivides two subcategories: category A and category B.

#### Category A

Radiation exposed worker, where the exposure to an effective dose of more than 6 mSv per year can be expected. [30, § 88] For Category A workers, the health suitability must be determined in an entrance- and annual screenings. [1, § 69]

The limit value of the effective dose is 20 mSv per calendar year. [30, § 4] However, it is custom practice that even at small deviations from the average monthly dose, enquiries are made.

#### Category B

Radiation exposed worker, who is expected to receive an effective dose of less than 6 mSv per year. [30, § 88]

---

<sup>1</sup>§ 3 (68) Strahlenexponierte Arbeitskraft: eine Person, die bei ihrer Arbeit im Rahmen einer unter die Bestimmungen dieses Bundesgesetzes fallenden Tätigkeit einer Exposition ausgesetzt ist und bei der davon auszugehen ist, dass sie Strahlendosen erhalten kann, die einen der für die Exposition der Bevölkerung festgelegten Dosisgrenzwerte übersteigen.

To secure compliance with the dose limit values, the LRP dictates a dose monitoring:

**§ 71 (1)** The dose of workers exposed to radiation must be determined systematically. The determination shall be made on the basis of individual measurements.<sup>2</sup> [1]

If, however, the dose for workers of category B can be estimated by other methods, the individual monitoring can be dropped. [30, § 100] Specifications for the requirements of individual monitoring are set in the GRPO:

**§ 98 (3)** Passive dosimeters, whose dose information cannot be deleted without special aids, must be used for dose assessment.<sup>3</sup> [1]

Passive dosimeters do not display the current dose and can therefore only be used to access the radiation dose received in retrospective. However, for some situations it is useful to have access to the current dose. For this, Electronic Personal Dosimeter (EPD) are used. The use of EPDs is common in radiation monitoring of pregnant women, as well as for high dose applications, where some APDs can even alert the wearer, as soon as a certain dose is exceeded.

## 4.2 Area monitoring

The measurement of the radiation fields in a certain area enables a dose estimation for an individual at a certain spot in advance. This ensures the compliance with radiation dose limits.

Radiation dose limits for general population are set in the GRPO:

**§ 6 (1)** For the sum of the annual exposures of an individual of the population from all activities, the limit values laid down in para. 2 and 3 apply.  
(2) The effective dose limit is one Millisievert per calendar year.<sup>4</sup> [1]

This corresponds to a dose of 20 µSv/week, which is used as the dose limit outside of radiation application rooms. In the course of a measurement report (Messgutachten) by an expert, the compliance with this limit is checked.

---

<sup>2</sup>§ 71 (1) Die Dosis strahlenexponierter Arbeitskräfte ist systematisch zu ermitteln. Die Ermittlung hat grundsätzlich anhand individueller Messungen zu erfolgen.

<sup>3</sup>§ 98 (3) Für die Dosiermittlung gemäß Abs. 1 und 2 sind passive Dosimeter zu verwenden, deren Dosisinformation nicht ohne spezielle Hilfsmittel gelöscht werden kann. Diese Dosimeter sind von der beauftragten Dosismessstelle zu beziehen und jeweils nach Ablauf eines Kalendermonats unverzüglich an diese zur Auswertung zu übermitteln.

<sup>4</sup>§ 6 (1) Für die Summe der jährlichen Expositionen einer Einzelperson der Bevölkerung aus allen Tätigkeiten gelten die in Abs. 2 und 3 festgelegten Grenzwerte.

(2) Der Grenzwert der effektiven Dosis beträgt ein Millisievert im Kalenderjahr.

## 4.3 Austrian legislation

According to § 7 of the Austrian Measurement- and Calibration Law<sup>5</sup> (MCL), measuring devices, whose accuracy is required by a legally protected interest, have to be officially calibrated.<sup>6</sup> Dosimeters for photon radiation used in radiation protection are covered by this regulation. Also, measurement devices for area monitoring in the course of expert opinions for official purposes (Gutachten) require officially calibrated devices. The official calibration of a device shall guarantee the compliance with certain error limits within the calibration interval. The specific error limits are hereby set in course of the admission. However, not all devices can be officially calibrated, regulations are set in the MCL:

**§ 38 (4)** Only measurement devices, or parts of measurement devices, whose physical basis and technical design ensure the accuracy and reliability of these measuring instruments, at least for the duration of the official calibration period specified for them, are allowed to be officially calibrated.

(5) The approval of the measurement devices, or parts of them, for official calibration, is based on the result of a detailed physical-technical examination.<sup>7</sup> [31]

An official calibration is valid until December 31<sup>st</sup>, 2 years after the official calibration process. For example, if a device is officially calibrated in January 2021 it is valid until December 31<sup>st</sup> 2023.

## 4.4 Detector types

Ionising radiation can not be measured directly but only via its interaction with matter. For radiation protection and dosimetry not only the detection of radiation fields, but also its quantification is important. For this various types of detectors are used, which can either work by the integrating or counting technique.

### Integrating technique

For example thermoluminescent dosimeter (TLD), film badge or quartz fibre dosimeter. Their function is based on the change of a physical parameter (e.g. voltage in a capacitor) by ionising radiation and the subsequent quantification of it. It is presumed, that the change of the specific physical parameter is proportional to the radiation dose. Due to their operating principle, no problems with pulsed ionising radiation are expected nor have been determined.

---

<sup>5</sup>Maß- und Eichgesetz

<sup>6</sup>In the German language and Austrian law a differentiation is made between "Kallibrierung" and "Eichung". While "Kallibrierung" is the quantification of the deviation from a norm "Eichung" is a official process where the compliance with certain error limits is checked. The measurement result of a measurement device which is "eichend" is considered correct before the law and can only be challenged with difficulty. Since the distinction between "Kallibrierung" and "Eichung" is not made in the English language, in this thesis the term "calibration" is used for "Kallibrierung" and for "Eichung" the term "official calibration" is used.

<sup>7</sup>§ 38 (4) Zur Eichung zuzulassen sind nur Meßgeräte oder Meßgeräteteile, deren physikalische Grundlage und technische Ausführung die Richtigkeit und Zuverlässigkeit dieser Meßgeräte mindestens für die Dauer der für sie festgelegten Nacheichfristen sicherstellen.

(5) Die Zulassung der Meßgeräte oder Meßgeräteteile erfolgt aufgrund des Ergebnisses einer eingehenden physikalisch-technischen Untersuchung.

However, all devices using the integrating technique share the disadvantage of making the radiation dose only accessible in retrospective, which is why they are also known as passive dosimeter. As explained in section 4.1 for some applications it can be useful or even necessary to have access to the current dose. Therefore, while passive dosimeter are used for individual monitoring required by the GRPO, dependent on the operational area, additional dosimeter which are able to display the current dose are used. Dosimeter capable of doing this are also known as active dosimeter and based on the counting technique.

Area monitoring, the quantification of a radiation field in a certain spot, is also only feasible with measurement devices using the counting technique.

## Counting technique

Measurement devices using the counting technique are based on the count of individual ionisation's and the subsequent electronic evaluation. Three popular devices using the counting technique are described in the following sections.

### 4.4.1 Ionisation chamber

Gas-filled ionisation detectors are the oldest devices used for the detection of ionising radiation. They are based on two electrodes in a gas-filled chamber. A typical technical implementation of an ionisation chamber is a counting tube. It is a cylindrical ionisation chamber with the tube serving as the cathode and a wire in the rotation axis as the anode.

When ionising radiation generates ions in the gas the freed electrons move towards the anode and cause a detectable voltage drop. The magnitude of this voltage drop is dependent on the amount of available electrons which in turn depend on the quantity and energy of the incident ionising radiation. Therefore, the measurement of the voltage allows conclusion to be drawn about the examined radiation field. Dependent on the applied voltage between the electrodes the detector can be operated at different modes.

The different operation modes are shown in figure 4.4.1:

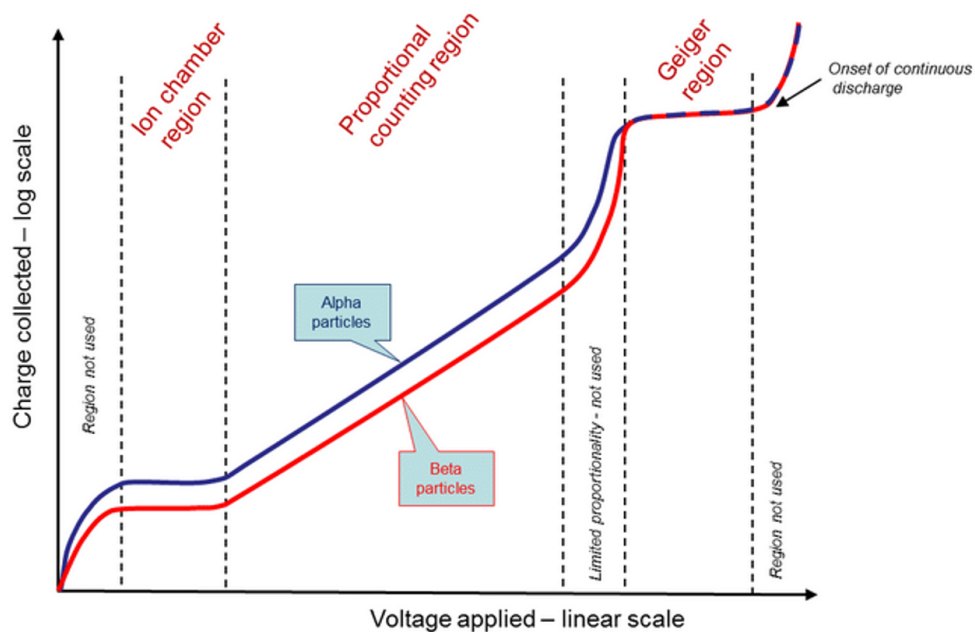


Figure 4.4.1: Operation modes of an ionisation chamber. [32]

The following operation modes are possible:

### Recombination

Due to the too low voltage and the resulting low acceleration the electrons recombine with the ions before reaching the anode. Only electrons initially close to the anode wire are detected, which does not allow any conclusion to be drawn about the total number of ionised particles.

### Ion chamber

With sufficient voltage all ionised electrons reach the anode. The number of liberated ions is proportional to the energy of the incoming ionising radiation. It must be kept in mind that the full energy of the examined radiation is only ascertainable if the total energy is deposited within the chamber.

### Proportional counter

With rising voltage the acceleration of the electrons is so high, that they themselves can cause further ionisation on their trajectory to the anode. This leads to an increase in measured electrons and therefore improves counting statistics.

### Geiger-Müller-Counter

At a certain point the acceleration of the electrons due to the voltage is so high that a single ionisation leads to a complete gas discharge. This is due to the avalanche of electrons and the emission of ultraviolet radiation which spreads the ionisation throughout the tube. However, due to the total discharge no conclusion about the energy of the incoming radiation can be made.

## 4.4.2 Scintillation counter

A scintillator is a object whose molecules can be excited by ionising radiation and emit energy in form of photons. In a scintillation counter these photons liberate electrons in a photocathode which then are multiplied by a photomultiplier and detected. The general scheme is shown in figure 4.4.2:

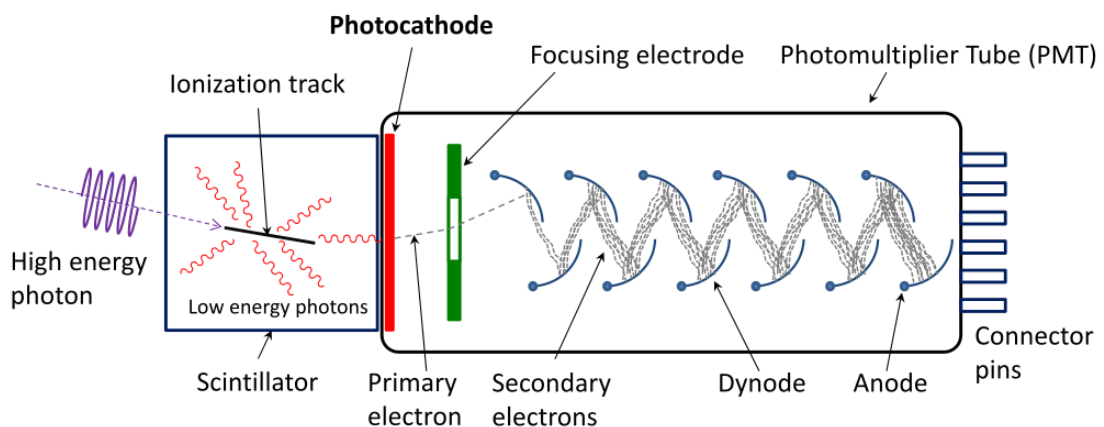


Figure 4.4.2: Function of a scintillation counter. [33]

Although multiple factors like the limited detection of low energy photons from the scintillator have to be considered, the measured current is proportional to the energy of the incoming radiation. The photomultipliers main purpose hereby is to enhance counting statistics.



### 4.4.3 Semi conductor

A pin-diode is a semi conductor electrical component consisting of three layers placed side by side, which are positively doped, undoped and negatively doped. The undoped layer is only intrinsically conductive, therefore the term positive-intrinsic-negative (pin) diode.

The function is based on the application of a voltage to the diode in the reverse direction. Photons with sufficient energy can produce electron-hole-pairs in the diode, which in turn travel to the similarly doped zones and induce a measurable current. Hereby, in the optimal case, the current is proportional to the energy of the photon.

Since they are based on it, detectors of this type are also often called semiconductor detectors.

## 4.5 Detection of pulsed radiation

In the case of pulsed fluoroscopy the dosimetric surveillance technique lagged behind the technological development and distribution. Oliver Hupe, expert for pulsed ionising radiation from the Physikalisch-Technische Bundesanstalt describes the situation as follows:

"Up to now, radiation protection dosimeters have only been tested in continuous fields, although they are used for measurements in pulsed radiation fields as well. Many of the conventional electronic dosimeters do not determine reliable dose values in these pulsed fields any more. The reasons for this are based on the measurement principle (mostly the counting technique) in combination with the characteristics of the pulsed radiation field (high dose rate during short radiation pulse)." [34, p. 1]

A large error potential in counting dosimeter is the effect of dead time  $t_d$ . After the detection of a particle a detector needs a minimum time until it is ready for another detection. This limits the number of detectable particles. For example, a detector with a dead time of 100  $\mu$ s can detect up to 10.000 particles/s at max.

The effect of dead time sets requirements for counting dosimeters when measuring pulsed radiation: [35]

If  $t_d \ll t_{\text{pulse}}$  the measuring device has to measure the dose rate of the pulse like a continuous dose rate.

If  $t_d \gg t_{\text{pulse}}$  the measuring device has to be able to measure the pulse dose correctly as a single pulse. The prerequisite is that the pulse frequency is lower than  $1/t_d$ .

In order to be able to assess the usability of a device in advance, knowledge of the pulse parameters is required.

Further potential problems, according to [26] are that it is unclear if a measurement device for dose or dose rate displays a maximum or average value. In most specifications of dosimeters this aspect is not addressed. Moreover, for short and intense radiation pulse the dose rate can be outside the measurement range of the device.

# Chapter 5

## Experimental setup

Due to the variety of applications of pulsed ionising radiation in medical imaging, a full address of all radiation sources is almost impossible. If one further considers the continuous use of the devices in normal patient operation, a longer-term interruption for experiments is neither in the interest of the medical institution nor the patients.

### 5.1 Radiation source

As an exemplary representative the C-arm "BV Pulsera" from Philips served as the radiation source for the comparative measurements. The manual describes its operational area as follows:

"BV Pulsera is a mobile X-ray system for the acquisition and visualisation of diagnostic X-ray images. It is intended for medical use in surgery." [36, 1-1]

The X-ray unit consisting of C-arm stand and a mobile viewing station is shown in figure 5.1.1:

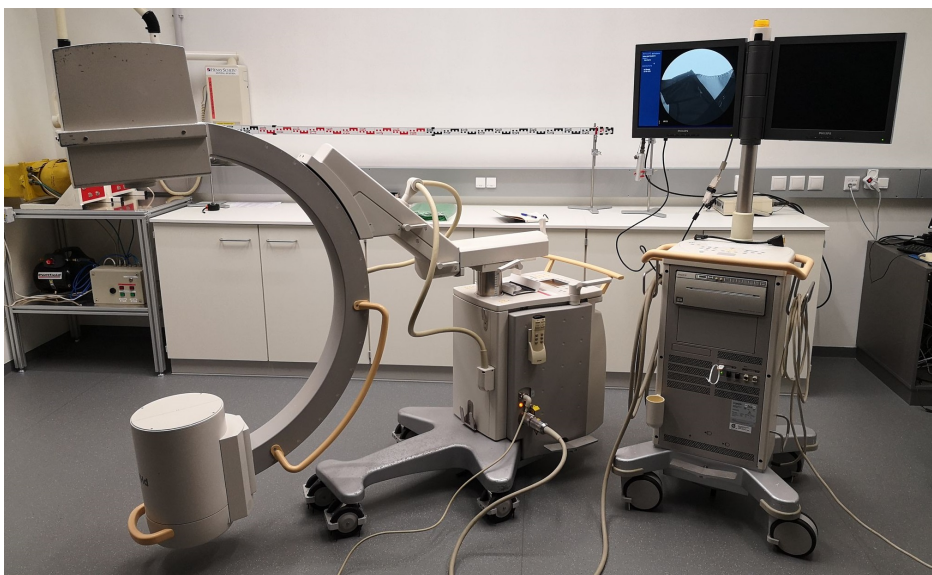


Figure 5.1.1: C-arm (left) and mobile viewing station (right).

C-arms are characterised by their variability in application and are regularly used with not transportable patients. The detector and X-ray tube are connected via an metal arc, whose orientation is highly adjustable. The mobility of the C-arm enables the adaption to the patient, instead of the opposite as usual. It is capable of doing single imaging as well as fluoroscopy with adaptable frames per second (fr/s), which is ideal for the intended measurements.

Despite the many customisable parameters, it must be noted that the results found in this thesis highly depend on the technical properties of this specific X-ray tube. This must be kept in mind when extrapolating the results on other radiation sources.

## 5.2 Radiation settings

Although usually the automatic dose rate control is used, and, as described in chapter 3 its availability is required by the MRPO, in this thesis manual control is necessary for ensuring continuous experimental conditions. However, due to the automatic coupling of kV and mA by the C-arm, the control is only half manual. The adaptable parameters of the measurements are:

- Examination type
- Radiation mode
- Pulse rate
- Voltage
- Exposure size of image intensifier
- Radiation time

The parameters are explained in the following sections in detail.

### 5.2.1 Examination type

The selected examination determines the framework conditions of the other settings. For example, a examination of bones, with high differences in density, does require other radiation settings than a *vascular examination* with a very low density gradient.

The following examinations are selectable:

- Abdominal
- Vascular
- Vascular CO2
- Vascular HQ
- Skeleton
- Head/Spine
- HQ Skeleton
- Thorax

The main influence of the chosen examination type is the current adjusted to the voltage. For example, the "HQ Skeleton" mode is achieved by an increase of the mA compared to the normal "Skeleton" mode.

## 5.2.2 Radiation mode

The radiation mode<sup>1</sup> sets the type of radiation emission. The following modes are choseable:

### **1/2 Dose**

Reduces radiation dose by using pulsed radiation instead of continuous. According to manual 12.5 Fr/s are acquired, own measurements resulted in 12.3 Fr/s.

### **1/4 Dose**

Analogous to the 1/2 dose mode. Instead of the 6 Fr/s stated in the manual 6.2 Fr/s were measured.

### **Dig. Image**

Used for single, high-quality images.

### **Pulsed**

Enables the independent selection of Fr/s. Hereby 3, 5 and 8 Fr/s can be chosen.

For the experiments the radiation mode "Pulsed" was chosen.

## 5.2.3 Pulse rate

The pulse rate can in the radiation mode "Pulsed" can be chosen individually. The selection of the frame rate was based on the results of the pre-measurements.

## 5.2.4 Voltage

The nominal voltage of the C-arm is specified as 120 kV. However, due to a technical limitation the maximal choseable voltage is 110 kV. In normal examination and therefore in this thesis as well, lower kV settings are used.

## 5.2.5 Exposure size of image intensifier

According to the optimisation principle it is useful to limit the radiation exposure solely on the examined body part. Therefore the exposition size of the image intensifier can be selected. The diameter can be set to 14, 17 or 23 cm, the detector housing itself has a diameter of 29.5 cm. Considering the elementary rule of conservatism in radiation protection, the biggest radius of 23 cm is chosen for all measurements.

## 5.2.6 Radiation time

The only continuous parameter of the measurement is the exposure time. The maximum exposition time according to manual is 30 s for all settings of pulsed radiation. Since the duration of the exposition has a fundamental influence on the measurable dose the exposition time is cited in every measurement.

---

<sup>1</sup>On the C-arm the mode can be chosen under the menu "Röntgen"

## 5.3 Measurement devices

In order to compare measurements, constant radiation settings have to be ensured. This is achieved with the diagnostic dosimeters RaySafe Unfors Xi and RaySafe Unfors X2. Due to their optimisation for varying radiation fields their results can be assumed to be correct.

The technical data of the reference dosimeter RaySafe Unfors Xi are stated in table 5.3.1, in figure 5.3.1 the base unit of the device (right) and its R/F <sup>2</sup> detector (left) are shown:



Figure 5.3.1: RaySafe Unfors Xi

Name	RaySafe Unfors Xi
Ser. number	191973 & 183686
Type	Semi conductor
Date of off. cal.	17.06.2019
Date of cal.	22.02.2019
Measured var.	Air kerma (rate)
Dose range	Not specified
Energy range	40 kV - 150 kV
Allowed error	5%

Table 5.3.1: Technical data RaySafe Unfors Xi

The RaySafe Unfors X2 is used particularly in the pre-measurements due to its ability of illustrating and measure the voltage curve. Its technical data is illustrated in table 5.3.2. In figure 5.3.2 its base unit (down), its R/F detector (left) and its area dose detector (right) are shown:



Figure 5.3.2: RaySafe Unfors X2

Name	RaySafe Unfors X2
Ser. number	257710 & 261004
Type	Semi conductor
Date of off. cal.	09.11.2020
Date of cal.	10.09.2018
Measured var.	Air kerma (rate)
Dose range	1 µGy - not specified
Dose rate range	0.3 µGy/s - 470 mGy/s
Energy range	40 kV - 150 kV
Allowed error	5%

Table 5.3.2: Technical data RaySafe Unfors X2

While the area dose detector was intended to serve as a standard for the measurements in the scattering radiation, its performance was insufficient.

<sup>2</sup>Radiography/Fluoroscopy

Main criterion for the tested measurement devices is the ability to officially calibrate the device in Austria. Therefore, even if not all devices were officially calibrated at the time of measurement they meet all requirements to be officially calibrated. Further attention was paid to the different technical structure and detector technique of the devices. A list of the tested measurement devices is shown in table 5.3.3

Device name	Abbreviation	Detector type	Calibrated	Officially calibrated
Szintomat 6134 A/H	Szintomat	Scintillator	Yes	Yes
6150 AD-b/E	AD-b	Scintillator	Yes	Yes
Umo LB123	Umo	Ionisation chamber	No	No
TOL/F LB1320	TOL/F	Ionisation chamber	Yes	Yes
6150 AD6/E	AD6	Geiger-Müller	Yes	Yes
GammaTwin	GammaTwin	Geiger-Müller	No	Yes
EPD Mk2	Mk2	Semi conductor	No	Yes
EPD TrueDose G	TruDose	Semi conductor	No	Yes
Rad-60SE	Rad-60	Semi conductor	No	Yes

Table 5.3.3: Tested devices

The AD-b is a scintillator tube used as an attachment for AD6. When connecting the two, only the scintillator is used for measurement. Therefore it is reckoned as a distinct measuring device, which has own properties and requires a separate official calibration.

Similarly, the Umo is usually only used by the Seibersdorf Labor GmbH in combination with a neutron probe. That is why it is not distinctly officially calibrated for area dose monitoring. However, since it meets all requirements for a official calibration and is used by other companies it is necessary to test its suitability for pulsed radiation.

In figure 5.3.3 all examined measuring devices, except the Rad-60, are shown:



Figure 5.3.3: All examined devices except the Rad-60. Lower row from left to right: AD6 with attached AD-b, Szintomat, Umo, TOL/F. Upper row from left to right: GammaTwin, Mk2, TruDose.

In the following sections the individual measuring devices are illustrated in detail.



### 5.3.1 Szintomat 6134 A/H

In figure 5.3.4 the Szintomat 6134 A/H is shown, in table 5.3.4 its technical data is illustrated:



Figure 5.3.4: Szintomat 6134 A/H

Name	Szintomat 6134 A/H
Ser. number	139087
Type	Scintillator
Date of off. cal.	16.11.2020
Date of cal.	16.11.2020
Measured var.	$H^*(10)$ and $\dot{H}^*(10)$
Dose range	0.05 $\mu\text{Sv}$ - 999.999 mSv
Dose rate range	0.1 $\mu\text{Sv/h}$ - 100 mSv/h
Energy range	28 keV - 7 MeV
Allowed error	< 10 $\mu\text{Sv(/h)}$ : 30% > 10 $\mu\text{Sv(/h)}$ : 20%

Table 5.3.4: Technical data Szintomat 6134 A/H

### 5.3.2 6150AD-b/E

In figure 5.3.5 the 6150AD-b/E is shown, in table 5.3.5 its technical data is illustrated:



Figure 5.3.5: 6150AD-b/E

Name	6150AD-b/E
Ser. number	112825
Type	Scintillator
Date of off. cal.	18.11.2019
Date of cal.	18.11.2019
Measured var.	$\dot{H}^*(10)$
Dose range	Not specified
Dose rate range	0.1 $\mu\text{Sv/h}$ - 100 $\mu\text{Sv/h}$
Energy range	20 keV - 7 MeV
Allowed error	< 10 $\mu\text{Sv(/h)}$ : 30% > 10 $\mu\text{Sv(/h)}$ : 20%

Table 5.3.5: Technical data 6150AD-b/E

### 5.3.3 GammaTwin

In figure 5.3.6 the GammaTwin is shown, in table 5.3.6 its technical data is illustrated:



Figure 5.3.6: GammaTwin

Name	GammaTwin
Ser. number	231535
Type	Geiger-Müller
Date of off. cal.	14.04.2020
Date of cal.	x
Measured var.	$H^*(10)$ and $\dot{H}^*(10)$
Dose range	0.5 $\mu$ Sv - 1.0 Sv
Dose rate range	0.5 $\mu$ Sv/h - 70 mSv/h
Energy range	45 keV - 1.3 MeV
Allowed error	30%

Table 5.3.6: Technical data GammaTwin

### 5.3.4 LB 123 Umo

In figure 5.3.7 the LB 123 Umo is shown, in table 5.3.7 its technical data is illustrated:



Figure 5.3.7: LB 123 Umo

Name	LB 123 Umo
Ser. number	6059
Type	Ion. chamber
Date of off. cal.	x
Date of cal.	x
Measured var.	$H_X$ and $\dot{H}_X$
Dose range	0.01 $\mu$ Sv - 1678 mSv
Dose rate range	0.05 $\mu$ Sv/h - 10 mSv/h
Energy range	30 keV - 1.2 MeV
Allowed error	< 10 $\mu$ Sv(/h): 30% > 10 $\mu$ Sv(/h): 20%

Table 5.3.7: Technical data LB 123 Umo

The Umo is used with the probe LB 1235 with the serial number 6068.



### 5.3.5 TOL/F LB 1320

In figure 5.3.8 the TOL/F LB 1320 is shown, in table 5.3.8 its technical data is illustrated:



Figure 5.3.8: TOL/F LB 1320

Name	Tol/F LB 130
Ser. number	6036
Type	Ion. chamber
Date of off. cal.	08.02.2021
Date of cal.	08.02.2021
Measured var.	$H_X$ and $\dot{H}_X$
Dose range	0.01 $\mu\text{Sv}$ - 300 mSv
Dose rate range	0.1 $\mu\text{Sv/h}$ - 10 mSv/h
Energy range	10 keV - 7 MeV
Allowed error	< 10 $\mu\text{Sv(/h)}$ : 30% > 10 $\mu\text{Sv(/h)}$ : 20%

Table 5.3.8: Technical data TOL/F LB 1320

The TOL/F is used with the probe LB 1321 with the serial number 6062.

### 5.3.6 6150AD6/E

In figure 5.3.9 the 6150AD6/E is shown, in table 5.3.9 its technical data is illustrated:



Figure 5.3.9: 6150AD6/E

Name	6159 AD 6/E
Ser. number	111414
Type	Geiger-Müller
Date of off. cal.	18.11.2019
Date of cal.	18.11.2019
Measured var.	$\dot{H}_X$
Dose range	Not specified
Dose rate range	0.5 $\mu\text{Sv/h}$ - 9.99 mSv/h
Energy range	60 keV - 1.3 MeV
Allowed error	< 10 $\mu\text{Sv(/h)}$ : 30% > 10 $\mu\text{Sv(/h)}$ : 20%

Table 5.3.9: Technical data 6150AD6/E

### 5.3.7 EPD Mk2

In figure 5.3.10 the EPD Mk2 is shown, in table 5.3.10 its technical data is illustrated:



Figure 5.3.10: EPD Mk2

Name	EPD Mk2
Ser. number	130582
Type	Semi conductor
Date of off. cal.	09.09.2019
Date of cal.	x
Measured var.	$H_p(10)$
Dose range	10 Sv - 10 Sv
Dose rate range	0.05 $\mu\text{Sv/h}$ - 1 Sv/h
Energy range	16 keV - 7 MeV
Allowed error	30%

Table 5.3.10: Technical data EPD Mk2

### 5.3.8 EPD TruDose G

In figure 5.3.11 the EPD TruDose G is shown, in table 5.3.11 its technical data is illustrated.



Figure 5.3.11: EPD TruDose G

Name	EPD Trudose
Ser. number	6111003
Type	Semi conductor
Date of off. cal.	10.11.2020
Date of cal.	x
Measured var.	$H_p(10)$
Dose range	10 Sv - 10 Sv
Dose rate range	0.1 $\mu\text{Sv/h}$ - 5 Sv/h
Energy range	16 keV - 7 MeV
Allowed error	20%

Table 5.3.11: Technical data EPD TruDose G

### 5.3.9 Rad-60SE

In figure 5.3.12 the Rad-60SE is shown, in table 5.3.12 its technical data is illustrated.



Name	Rad-60SE
Ser. number	283111
Type	Semi conductor
Date of off. cal.	11.02.2021
Date of cal.	x
Measured var.	$H_p(10)$
Dose range	10 Sv - 10 Sv
Dose rate range	0.05 $\mu\text{Sv/h}$ - 3 Sv/h
Energy range	55 keV - 3 MeV
Allowed error	30%

Table 5.3.12: Technical data Rad-60SE

Figure 5.3.12: Rad-60SE

## 5.4 Experimental geometry

In order to accomplish comparable results not only the radiation settings, but also the experimental geometry must be kept constant.

The first main variable is the orientation and positioning of the C-arm. For the measurements an overhead radiation set up is used, meaning the X-ray tube is located above the detector. This enables the placement of the measuring devices, respectively the scattering body, on the detector. Due to the connection of X-ray tube and detector in the C-arm setup, the precise positioning of one automatically determines the position of the other. The distance from the floor to the upside of the detector was set at 70 cm. The orientation of the C-arm was checked with the marks on the C-arm itself and a bubble level on the surface of the detector.

With the main orientation of the C-arm being fixed, the other specifics of the experimental setup are determined by the two examined radiation fields: the stray- and useful radiation.

### 5.4.1 Stray radiation

In radiation protection the radiation scattered by the patient plays an important role. The *half value layer thickness* for 70 kV X-ray in soft tissue is about 3 cm. [37] Assuming a slim patient with a abdomen diameter of 21 cm, this results in the weakening of radiation intensity during the transition through the patient to less than 1% of the initial intensity. While some energy is deposited in the patient as radiation dose, the majority is scattered.

The angle distribution of stray radiation must not be mistaken with the angle distribution of single interactions as described in section 1.2.3. Due to the high absorption within the patient, the most intense stray radiation field is in a  $45^\circ$  back scatter angle, as shown in figure 5.4.1:

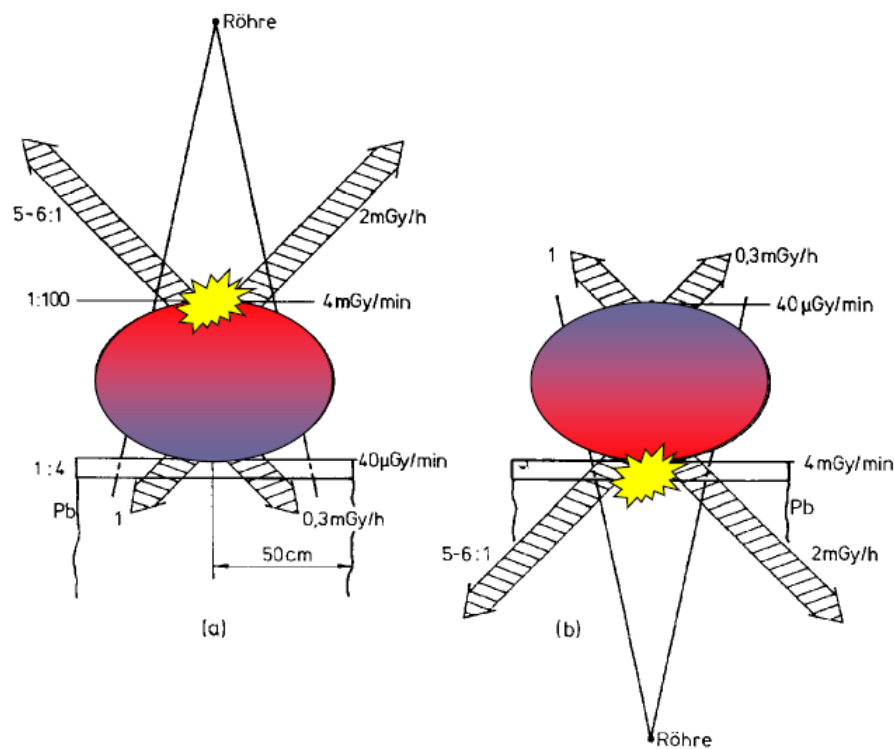


Figure 5.4.1: Scattered radiation field of an X-ray tube at 70 kV. [37, p. 4]

Simulating the patient is a water phantom with dimensions of 25 cm x 25 cm x 15 cm. This phantom is placed centred on the detector. The Unfors is positioned on the phantom in order to check the consistency of radiation conditions. The tested measurement devices are placed on the same height as the phantom, in a  $90^\circ$  angle to the C-arm connection of X-ray tube and detector, as shown in figure 5.4.2

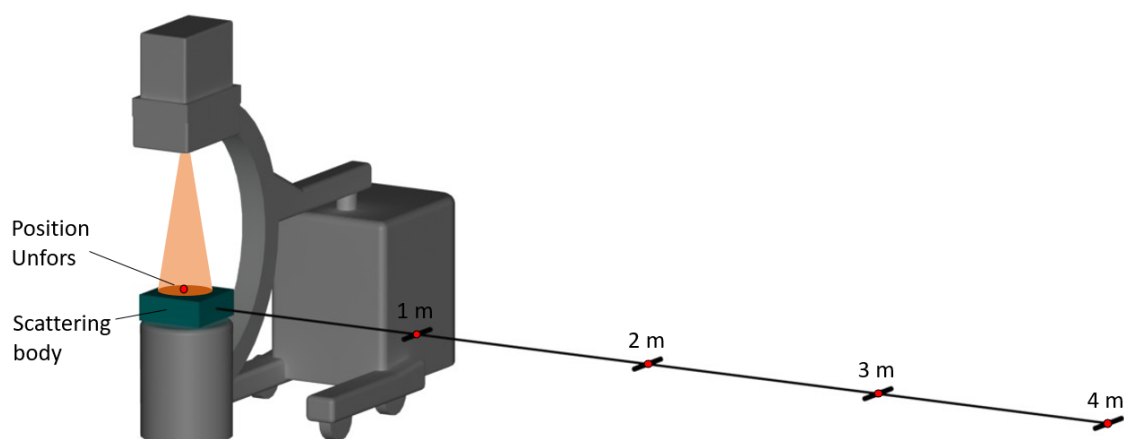


Figure 5.4.2: Experimental setup for stray radiation.

In total four measurement positions were used in 1, 2, 3 and 4 m distance from the centre of the scattering body. Since in the calibration of the EPDs back scattered radiation is factored in, they were fixed to another scattering body for the measurements.

## 5.4.2 Useful radiation

Useful radiation is understood to mean the part of the beam, that is used for imaging. Due to the high dose rate within the beam a correct measurement is especially important. The Unfors and the individually examined measurement device are placed on a lead plate protecting the image intensifier from long intense radiation. The experimental setup is shown in figure 5.4.3:

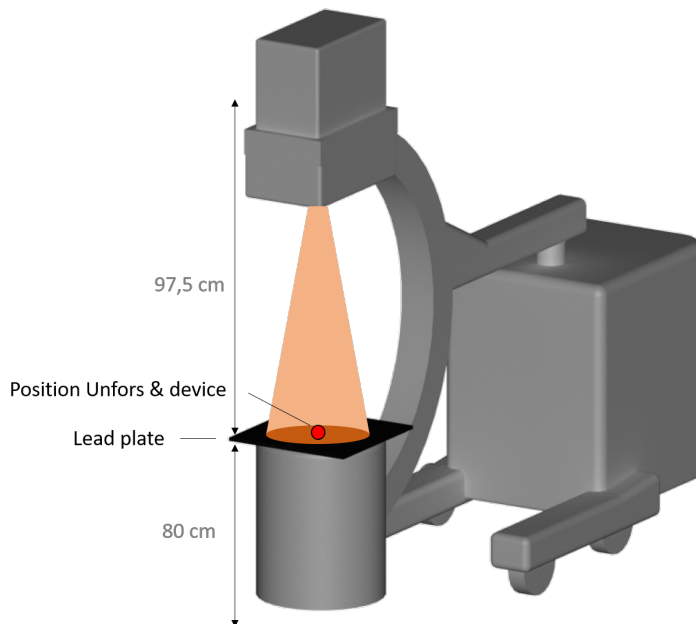


Figure 5.4.3: Experimental setup for useful radiation.

The specified distances describe the distance from the ground to the detector surface and from the detector surface to the focus point of the X-ray tube.

Analogues to the measurements in the scattering field, the EPDs were fixated on a scattering body for the measurements in the useful radiation. In this setup the lead plate was not in use.

An image of the positioning of the EPDs and the Unfors can be seen in figure 5.4.4

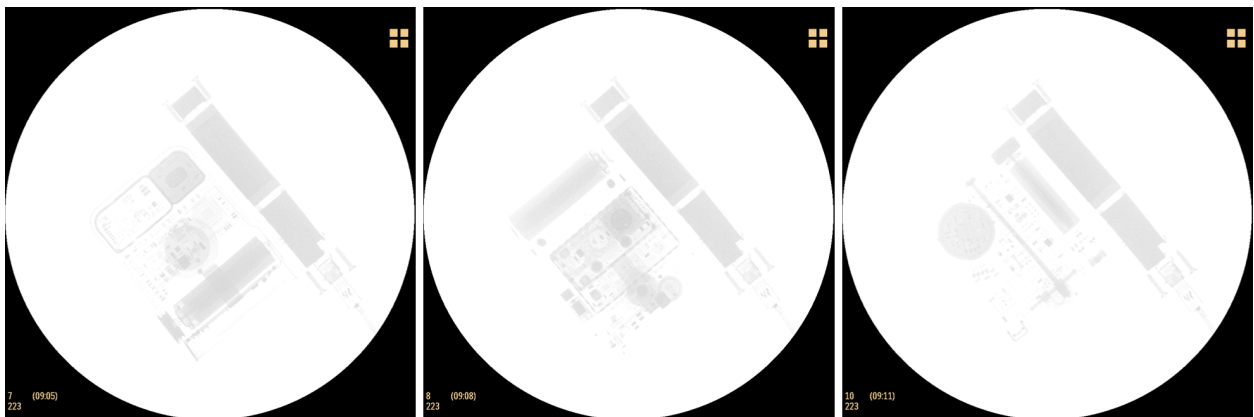


Figure 5.4.4: The EPDs and Unfors in the useful beam. From left to right: Mk2, TruDose, Rad-60.

The images were taken with the preselected 90 kV which is not the optimal voltage for imaging these detectors, hence the paleness.

# Chapter 6

## Results

Before the main measurements, the proper function of the C-arm and Unfors had to be checked. Furthermore, the radiation parameter had to be established in the course of pre-measurements. After the successful verification, the measurements in the stray- and useful radiation could be carried out. In the following chapter the results of the pre- and main measurements are illustrated and interpreted.

### 6.1 Pre-measurements

In order to carry out comparative measurements of different measuring devices, the radiation settings have to be determined. The pulse properties of the various radiation settings are found by pre-measurements.

The examination type "Vascular HQ" with 80 kV in the mode "Pulsed" was chosen for the pre-measurements. The pulse properties were measured with the Unfors X2, the results are illustrated in table 6.1.1:

Set fr/s	Current [mA]	Voltage [kV]	Duration [s]	Dose [ $\mu$ Gy]
3	1.85	79.0	11.34	569.2
5	3.14	78.7	10.21	842.8
8	4.66	78.4	10.27	1260
Dose r. [ $\mu$ Gy/s]	Dose/pulse [ $\mu$ Gy]	Pulses	Pulses/s	$t_{\text{pulse,base}}$ [ms]
48.92	16.3	35	3	12.1
81.38	16.3	52	5	15.9
121.5	16.2	78	7.5	14.0

Table 6.1.1: Pulse properties at different frame rates.

Only the set fr/s and the automatically adapted current are set values. All other data given in table 6.1.1 are measured. The constant dose/pulse results in a linear relation between Fr/s and dose rate. The apparent contradiction between the set 8 fr/s and measured 7.5 fr/s is in accordance with the manual. The selection probably only shows 8 fr/s due to difficulties with displaying decimals on the screen.



The pulse base duration was measured with the help of the measuring mode of the Unfors XII, which is able to illustrate the voltage curve, as shown in figure 6.1.1 and 6.1.2:

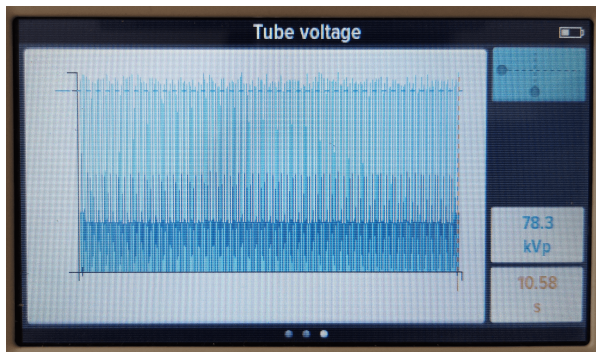


Figure 6.1.1: Voltage curve large view.

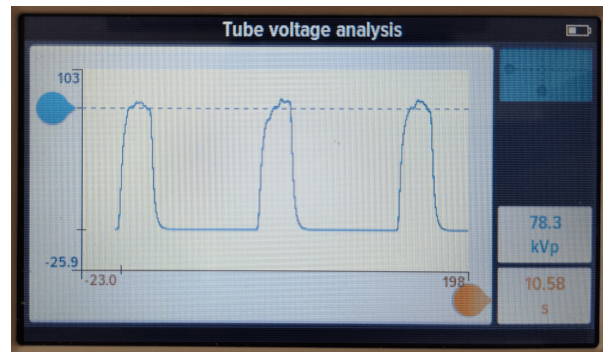


Figure 6.1.2: Voltage curve detail view.

For the pulse base duration three pulses were measured and averaged. The measured pulse duration is in contrast to the manual which states a constant pulse width of 13 ms, regardless of the chosen fr/s. However, no specifications are made if the specified duration is  $t_{\text{pulse,base}}$ ,  $t_{\text{pulse}}$  or  $t_{\text{pulse,plateau}}$ . Furthermore, the manual measuring with the voltage curve is probably too inaccurate and the averaging over three pulses too little. Therefore, despite the measurement results, a constant pulse duration is assumed for all frame rates.

Based on the constant pulse width and constant dose/pulse it was decided to carry out the experiments in the stray and useful radiation at 8 fr/s due to the higher dose and better counting statistics.

## 6.2 Stray radiation

When carrying out experiments with ionising radiation, care must be taken to ensure adequate self-protection, which is why a lead vest was worn during all measurements. Furthermore, the exposure time was reduced by measuring multiple devices simultaneously. The examined measuring devices were lined up along the edge of a table, as shown in figure 6.2.1:



Figure 6.2.1: Setup of the measuring devices.

Attention was paid to ensure that the measuring chambers were all at the same height. All experiments were carried out at the same radiation setting:

- **Examination type:** Vascular HQ
- **Radiation mode:** Pulsed
- **Pulse rate:** 8 Fr/s
- **Voltage:** 90 kV (4.76 mA)
- **Exposure size image int.:** 23 cm
- **Radiation time:** 30 s

Analogous to the pre-measurements the mode "Vascular HQ" in the mode "Pulsed" was chosen. However, the voltage was increased to 90 kV which is common for C-arm applications and generates a sufficient radiation dose while not overloading the X-Ray tube in the long term. Due to an automatic interruption of radiation output after 30 s, it was set as the radiation time.

The devices were tested in three series of measurements:

**Series 1:** AD6, Szintomat, GammaTwin

**Series 2:** AD-b, TOL/F, Umo

**Series 3:** Mk2, TruDose, Rad-60

During the radiation exposure the dose rates displayed by the devices were steadily noted. This way, despite the fluctuations, an average value, including errors, can be given for the dose rates. The dose is automatically summed up from the dose rate and exposure time and displayed by the devices. According to this the dose always refers to an exposure time of 30 s.

The devices for the measurement series were arranged on the basis of space availability. However, only measurement devices with the same measurement parameter are directly comparable. To compare devices from different measurement series it has to be ensured, that the radiation parameter stayed constant over all measurements. The voltage, dose rate and radiation time of all three measurement series, measured with the 'Unfors', are shown in table 6.2.1:

Meas. Series	Series 1			
Voltage [kV]	89.4	89.7	89.1	89.1
Dose rate [ $\mu$ Gy/s]	246.4	246.6	247.0	246.5
Radiation time [s]	29.87	30.0	29.87	30.0
Meas. Series	Series 2			
Voltage [kV]	89.3	89.5	89.5	89.1
Dose rate [ $\mu$ Gy/s]	248.1	248.0	247.9	247.1
Radiation time [s]	29.87	29.87	29.87	29.87
Meas. Series	Series 3			
Voltage [kV]	90.83	90.91	90.77	90.65
Dose rate [ $\mu$ Gy/s]	245.6	246.8	245.2	250.0
Radiation time [s]	29.57	29.97	29.97	29.97

Table 6.2.1: Voltage, dose rate and radiation time in the useful beam of all measurements in the stray radiation

Considering all 12 measurements, the average energy in the useful beam is  $(89.8 \pm 0.7)$  kV<sup>1</sup>. The dose rates average is  $(247.1 \pm 1.3)$  Gy/s. The average radiation time is  $(29.89 \pm 0.11)$  s. With the relative errors of 0.8%, 0.5% and 0.4% being much smaller than the deviations of the dose values measured by the tested devices, the emitted radiation can be considered constant.

<sup>1</sup>By default, the standard deviation is specified as the error



### 6.2.1 $H^*(10)$ devices

Devices whose measured variables are  $H^*(10)$  and  $\dot{H}^*(10)$  are called category 1 devices in this thesis. These are the Szintomat (scint.), AD-b (scint.) and GammaTwin (Geiger-Müller).

The dose and dose rate results are illustrated in table 6.2.2:

Position	1 m	2 m	3 m	4 m
Szintomat dose rate [ $\mu\text{Sv/h}$ ]	$700 \pm 50$	$110 \pm 5$	$65 \pm 5$	$40 \pm 5$
Szintomat dose [ $\mu\text{Sv}$ ]	$5.37 \pm 0.01$	$1.23 \pm 0.01$	$0.53 \pm 0.01$	$0.30 \pm 0.01$
AD-b dose rate [ $\mu\text{Sv/h}$ ]	99.9 (max out)	99.9 (max out)	$95 \pm 5$	$55 \pm 5$
AD-b dose [ $\mu\text{Sv}$ ]	$1.40 \pm 0.01$	$1.33 \pm 0.01$	$0.83 \pm 0.01$	$0.48 \pm 0.01$
GammaTwin dose rate [ $\mu\text{Sv/h}$ ]	$430 \pm 10$	$155 \pm 5$	$82 \pm 2$	$50 \pm 2$
GammaTwin dose [ $\mu\text{Sv}$ ]	$3.52 \pm 0.01$	$1.32 \pm 0.01$	$0.69 \pm 0.01$	$0.43 \pm 0.01$
Average dose [ $\mu\text{Sv}$ ]	3.43	1.29	0.68	0.40
Standard deviation [ $\mu\text{Sv}$ ]	1.99	0.05	0.15	0.09

Table 6.2.2: Dose measurement results category 1 devices.

Due to the analogue logarithmic display of the Szintomat its error is proportional to the chosen measuring range. According to manual, the AD-b maxes out at a dose rate of  $100 \mu\text{Sv/h}$ , which was confirmed by the measurements. The AD-b and GammaTwin have nearly matching dose values at 2 m, despite divergent dose rate values. Hereby, the time span until the maximum dose rate is achieved has to be taken into account. Since the AD-b reaches the maximum dose rate faster than the GammaTwin it can still yield the same dose value.

In figure 6.2.2 the measured dose values are visualised. Hereby, the data points of 2, 3 and 4 m were fitted with the function  $a/x^2$  and extrapolated to 1 m:

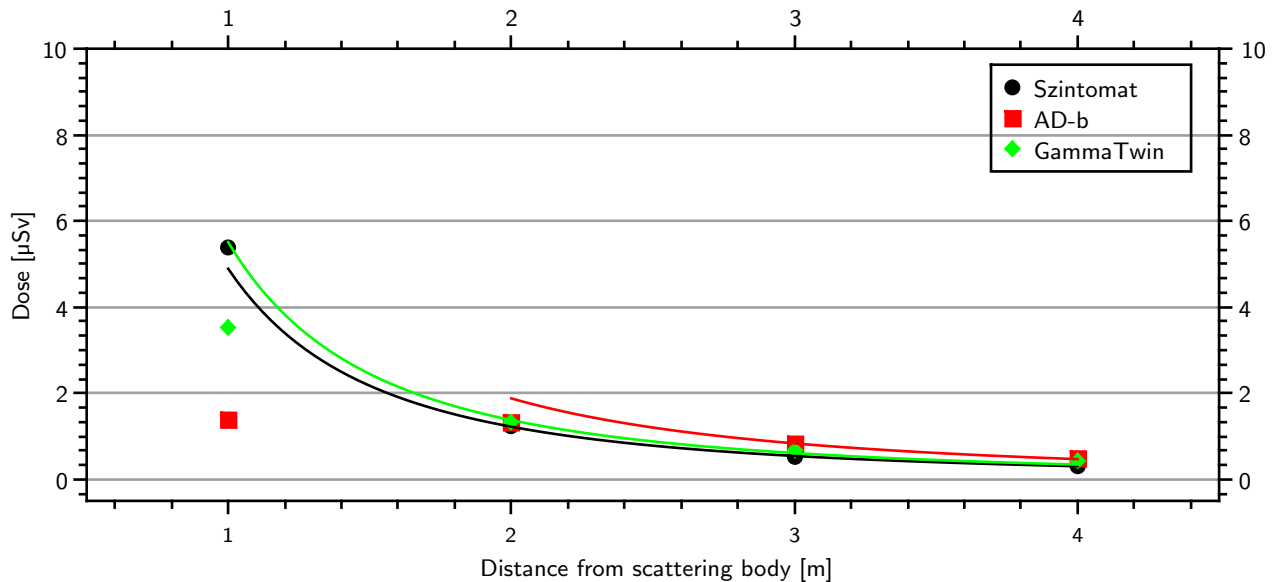


Figure 6.2.2: Dose measurements results category 1 devices.

The Szintomat follows the square course best. The AD-b was only fitted to a distance of 2 m due to its maxing out. Error bars were not integrated in the plot because they are too small to be seen.

## 6.2.2 $H_x$ devices

Devices whose measured variables are  $H_x$  and  $\dot{H}_x$  are called category 2 devices in this thesis. These are the Umo (ion-chamb.), TOL/F (ion-chamb.) and AD6 (Geiger-Müller).

The dose and dose rate results are illustrated in table 6.2.3:

Position	1 m	2 m	3 m	4 m
Umo dose rate [ $\mu\text{Sv/h}$ ]	$180 \pm 2$	$45 \pm 1$	$20 \pm 1$	$12 \pm 1$
Umo dose [ $\mu\text{Sv}$ ]	$1.48 \pm 0.01$	$0.38 \pm 0.01$	$0.18 \pm 0.01$	$0.10 \pm 0.01$
TOL/F dose rate [ $\mu\text{Sv/h}$ ]	$615 \pm 15$	$153 \pm 5$	$72 \pm 3$	$43 \pm 1$
TOL/F dose [ $\mu\text{Sv}$ ]	$5.10 \pm 0.01$	$1.29 \pm 0.01$	$0.61 \pm 0.01$	$0.35 \pm 0.01$
AD6 dose rate [ $\mu\text{Sv/h}$ ]	$310 \pm 5$	$110 \pm 1$	$50 \pm 1$	$31 \pm 1$
AD6 dose [ $\mu\text{Sv}$ ]	$2.61 \pm 0.01$	$0.91 \pm 0.01$	$0.42 \pm 0.01$	$0.26 \pm 0.01$
Average dose [ $\mu\text{Sv}$ ]	3.06	0.86	0.40	0.24
Standard deviation [ $\mu\text{Sv}$ ]	1.85	0.46	0.21	0.12

Table 6.2.3: Dose measurements results category 2 devices.

The measured doses of category 2 devices diverge at all distances. However, it is remarkable, that for the distances from 2 to 4 m the standard deviation grows in the same ratio as the average dose. According to this the ratio of standard deviation and average dose with values of 53% (2 m), 53% (3 m) and 50% (4 m) nearly stays constant. At 1 m distance the relative error is 60%, which corresponds to the overall trend.

In figure 6.2.3 the measured dose values are visualised:

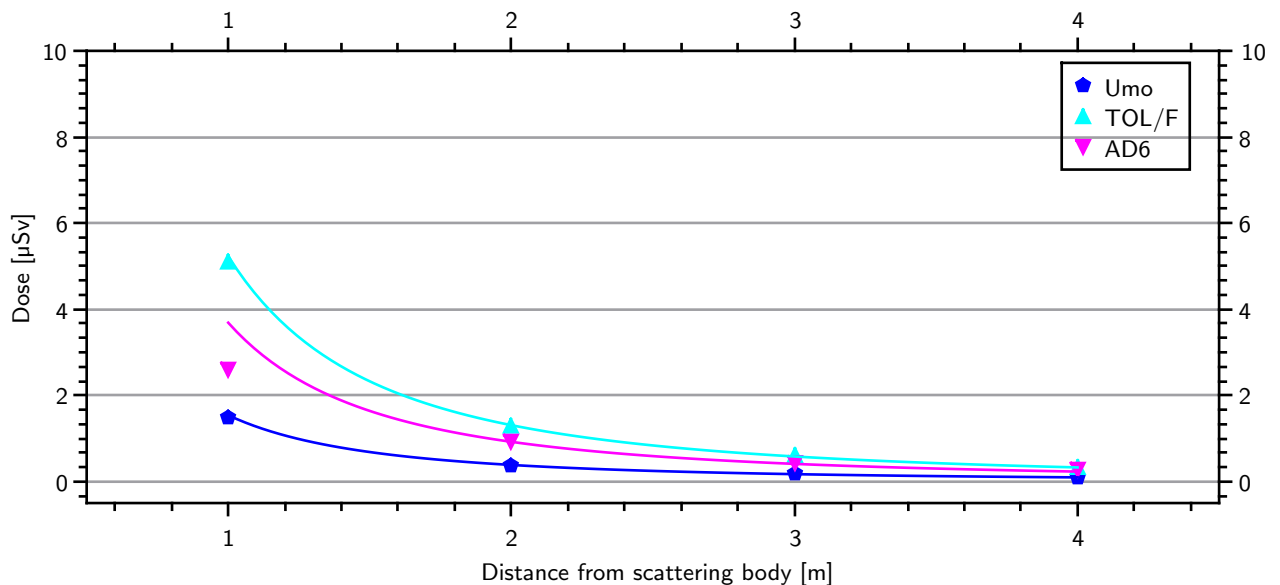


Figure 6.2.3: Dose measurements results category 2 devices.

In the plot the parallelism of lines is noticeable. The TOL/F consistently measures the highest dose, the Umo the lowest. While the Umo and TOL/F follow the square course even in 1 m distance, the AD6 diverges from it. Furthermore, the already observed proportional increase in average dose and standard deviation can be seen.

### 6.2.3 $H_p(10)$ devices

Devices whose measured variables are  $H_p(10)$  and  $\dot{H}_p(10)$  are called category 3 devices in this thesis. These are the Mk2, TruDose and Rad-60 (all Semi conductor).

The dose and dose rate results are illustrated in table 6.2.4:

Position	1 m	2 m	3 m	4 m
Mk2 dose [ $\mu\text{Sv}$ ]	$8 \pm 1$	$1 \pm 1$	$0 \pm 1$	$0 \pm 1$
TruDose dose [ $\mu\text{Sv}$ ]	$9.6 \pm 0.1$	$2.3 \pm 0.1$	$1.0 \pm 0.1$	$0.6 \pm 0.1$
Rad-60 dose [ $\mu\text{Sv}$ ]	$3 \pm 1$	$1 \pm 1$	$1 \pm 1$	$0 \pm 1$
Average dose [ $\mu\text{Sv}$ ]	6.86	1.43	0.67	0.20
Standard deviation [ $\mu\text{Sv}$ ]	3.44	0.75	0.58	0.35

Table 6.2.4: Dose measurements results category 3 devices.

All devices share the display of the dose by default. The display of the dose rate can be selected, but after around 5 seconds it automatically jumps back to the display of the dose. Therefore, for these devices, no dose rate could be documented.

Especially at greater distances the results vary widely. This mainly can be attributed to the fact, that the Mk2 and Rad-60 can only display integer numbers for the dose. Therefore, in the far field with low doses, they behave binary.

In figure 6.2.4 the measured dose values are visualised:

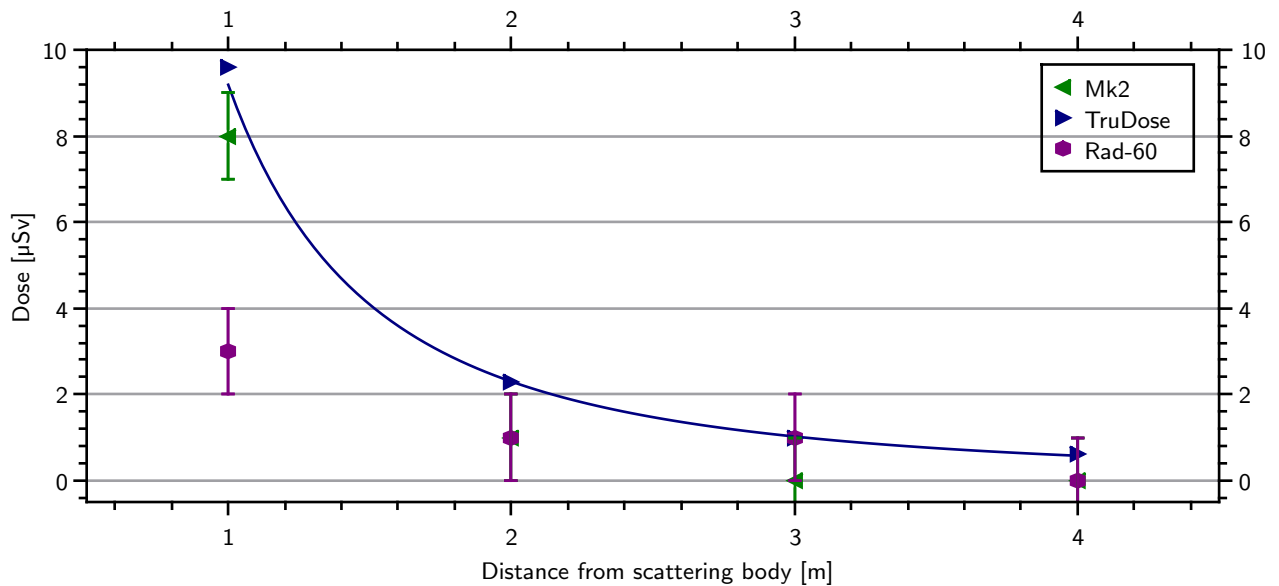


Figure 6.2.4: Dose measurements results category 3 devices.

In contrast to the plots of category 1 and 2 devices, the plot of category 3 devices is characterized by hard transitions. It is assumed that the dose results are not rounded by the devices. So, for example, if the Mk2 measures a dose of  $1.9 \mu\text{Sv}$  it will still display  $1 \mu\text{Sv}$ . Therefore, the upper half of the error bars is particularly relevant. Due to their binary behaviour the Mk2 and Rad-60 were not fitted.

## 6.2.4 Comparison of categories

First of all, the consistency of the measurement devices within a category is checked. In figure 6.2.5 the average dose and standard deviation of each category are illustrated:

Position	1 m	2 m	3 m	4 m
Category 1 average dose [ $\mu\text{Sv}$ ]	3.43	1.29	0.68	0.40
Category 1 standard deviation [ $\mu\text{Sv}$ ]	1.99	0.05	0.15	0.09
Category 2 average dose [ $\mu\text{Sv}$ ]	3.06	0.86	0.40	0.24
Category 2 standard deviation [ $\mu\text{Sv}$ ]	1.85	0.46	0.21	0.12
Category 3 average dose [ $\mu\text{Sv}$ ]	6.86	1.43	0.67	0.20
Category 3 standard deviation [ $\mu\text{Sv}$ ]	3.44	0.75	0.58	0.35

Table 6.2.5: Averaged dose measurement results of all categories.

Category 3 devices have throughout the highest standard deviation, whereby the integer display of the Mk2 and Rad-60 has to be taken into account. Also, in distances of 2 m and closer, the category 3 devices measure on average more than double of the categories 1 and 2.

Except at 1 m, the category 1 devices have the lowest standard deviation. The higher deviation at 1 m can primarily be accounted to the maxing out of the AD-b.

As explained in section 1.4.2 the results of devices measuring different measurement variables are not directly comparable. However, with the help of conversion factors an approximation is made. The main parameter for the conversion is the energy of the radiation. According to [38] the effective photon energy is approximately equal to between one third and half of the maximum photon energy. If one considers the high filtration of the C-arm with 6,7 mm Al and the according energy shift in the spectrum to higher energies, an effective photon energy of 45 keV is assumed. The conversion factors are illustrated in figure 6.2.5:

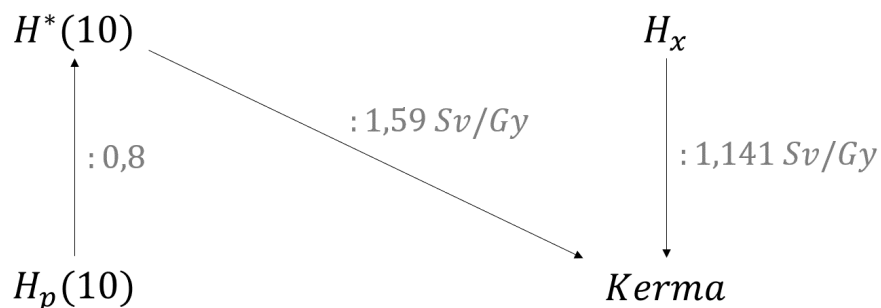


Figure 6.2.5: Conversion factors between measurement variables. [39, p. 26, 35, 217]

The conversion factors between  $H_p(10)$  and  $H^*(10)$  refers to a energy of 50 kV. The conversion for  $H^*(10)$  refers to a energy of 48 kV. Although the deviations coming from this are expected to be small, it should be kept in mind.

The conversion factor from  $H_x$  to kerma on the other hand is a fixed value for energies below 3 MeV [39, p. 217]

In table 6.2.6 the measured doses of all measurement devices in the converted unit  $\mu\text{Gy}$  are illustrated:

Position	1 m	2 m	3 m	4 m
Szintomat [ $\mu\text{Gy}$ ]	3.38	0.77	0.33	0.19
AD-b [ $\mu\text{Gy}$ ]	0.88	0.84	0.52	0.30
GammaTwin [ $\mu\text{Gy}$ ]	2.21	0.83	0.43	0.27
Umo [ $\mu\text{Gy}$ ]	1.30	0.33	0.16	0.09
TOL/F [ $\mu\text{Gy}$ ]	4.47	1.13	0.53	0.31
AD6 [ $\mu\text{Gy}$ ]	2.29	0.80	0.37	0.23
Mk2 [ $\mu\text{Gy}$ ]	6.37	0.8	0	0
TruDose [ $\mu\text{Gy}$ ]	7.64	1.83	0.80	0.48
Rad-60 [ $\mu\text{Gy}$ ]	2.39	0.80	0.80	0

Table 6.2.6: Dose measurement results of all devices in  $\mu\text{Gy}$ .

Due to the multiplication with a constant factor the functions of the devices are just shifted. According to the conversion factors the values are 37% (category 1), 12% (category 2) or 20% (category 3) lower than in their original unit. One must be aware, that comparing converted values is difficult, because the conversion factors assume certain ideal radiation qualities. Since the exact potential error is difficult to quantify none was given in table 6.2.6. However, the majority of statements in the comparison of devices of different categories is based on comparing the curve shapes, not the specific values.

In figure 6.2.6 all measurement devices with categorisation in measurement variable are visualised:

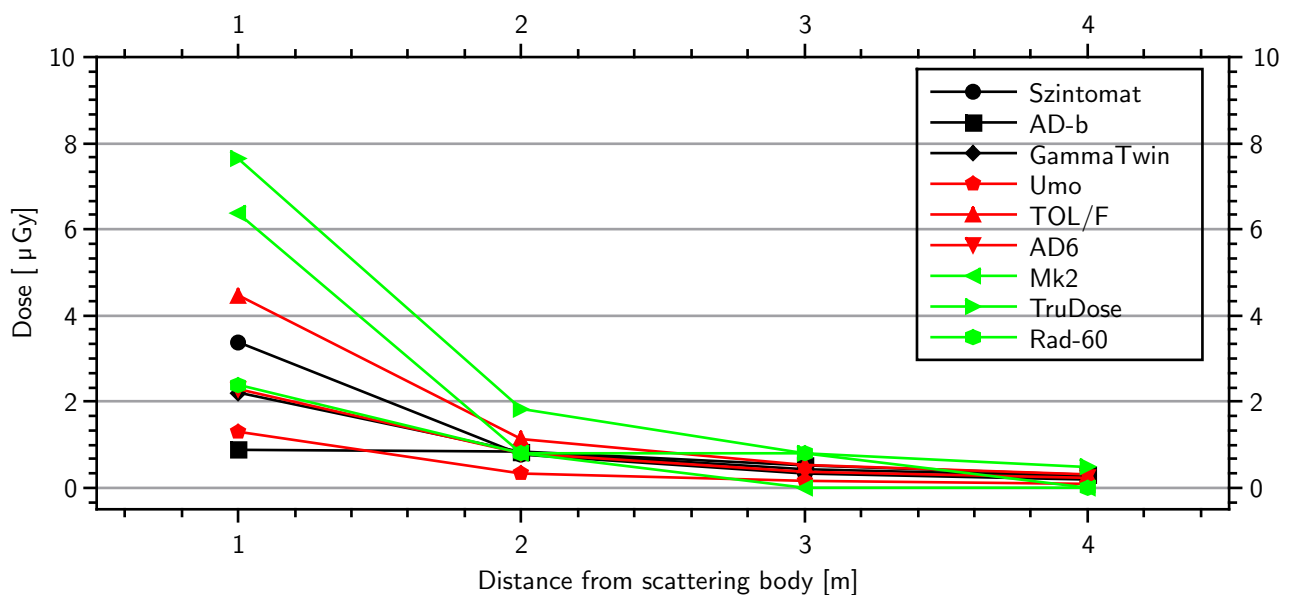


Figure 6.2.6: Dose measurement results of all devices. Category 1 devices in black, category 2 devices in red, and category 3 devices in green.

Firstly, the tendency to high dose values of the EPDs leaps to the eye. Especially the TruDose and Mk2 distinctly measure higher doses than the other measurement devices.

Furthermore, it is interesting how the functions of category 1 and 2 devices have a similar course with the splitting up at 1 m. The category 2 devices however already split up before as explained in section 6.2.2 while the category 1 devices measure very similar values up to a distance of 2 m.

## 6.2.5 Comparison of detector type

In this section a possible correlation between measurement stability and detector type is checked. In table 6.2.7 the average dose and standard deviation results, categorised according to detector type, are illustrated:

Position	1 m	2 m	3 m	4 m
Scintillator average dose [ $\mu\text{Gy}$ ]	2.13	0.81	0.43	0.25
Scintillator standard deviation [ $\mu\text{Gy}$ ]	1.77	0.05	0.13	0.08
Ionisation chamber average dose [ $\mu\text{Gy}$ ]	2.25	0.82	0.40	0.25
Ionisation chamber standard deviation [ $\mu\text{Gy}$ ]	0.06	0.02	0.04	0.03
Geiger-Müller average dose [ $\mu\text{Gy}$ ]	3.07	1.12	0.56	0.35
Geiger-Müller standard deviation [ $\mu\text{Gy}$ ]	0.64	0.29	0.19	0.12
Semi conductor dose [ $\mu\text{Gy}$ ]	5.47	1.14	0.53	0.16
Semi conductor standard deviation [ $\mu\text{Gy}$ ]	2.74	0.59	0.46	0.28

Table 6.2.7: Dose measurement results of all detector types.

The ionisation chambers have by far the lowest standard deviation in all measurement points. The EPDs on the other hand have the highest at all points.

However, due to the small number of detectors in each category (2, 2, 2 and 3) no general statements regarding the consistency or reliability of each detector type can be made.

In figure 6.2.7 all measurement devices with categorisation in detector type are visualised:

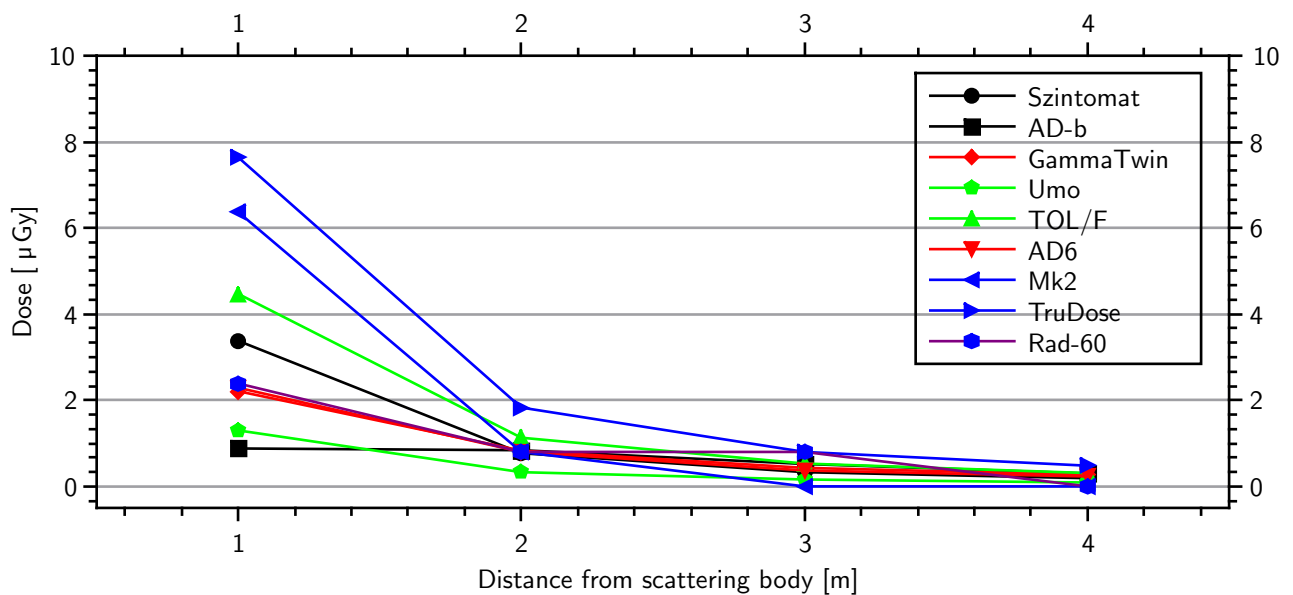


Figure 6.2.7: Dose measurement results of all detector types. Scintillators in black, Geiger-Müller counter in red, ionisation chamber in green and pin diodes in blue.

Due to the excellent accordance of the GammaTwin and AD6 the lines can not be distinguished.

As can be seen in the plot, due to the maxing out of the AD-b the results for the scintillators in table 6.2.7 are automatically distorted.

## 6.2.6 Comparison of all devices

Lastly, it is investigated, whether general statements about the reliable use of measuring instruments in pulsed radiation fields can be derived from the data.

In table 6.2.8 the overall average dose and standard deviation are illustrated:

Position	1 m	2 m	3 m	4 m
Average dose [ $\mu\text{Gy}$ ]	3.44	0.90	0.44	0.21
Standard deviation [ $\mu\text{Gy}$ ]	2.30	0.40	0.27	0.16

Table 6.2.8: Averaged dose measurement results of all devices.

Interestingly, the measured dose values seem to converge at a distance of 2 m. If the Umo and TruDose are considered as outliers and ignored, the average dose value is  $0.86 \mu\text{Gy}$  with a standard deviation of  $0.12 \mu\text{Gy}$ . The dose rate in a distance of 2 m seems to be in an area, where the majority of measurement devices works well. At further distances the dose rate is too small for some devices, at closer distances they split up drastically.

In figure 6.2.8 the measured doses in the stray radiation of all devices are visualised:

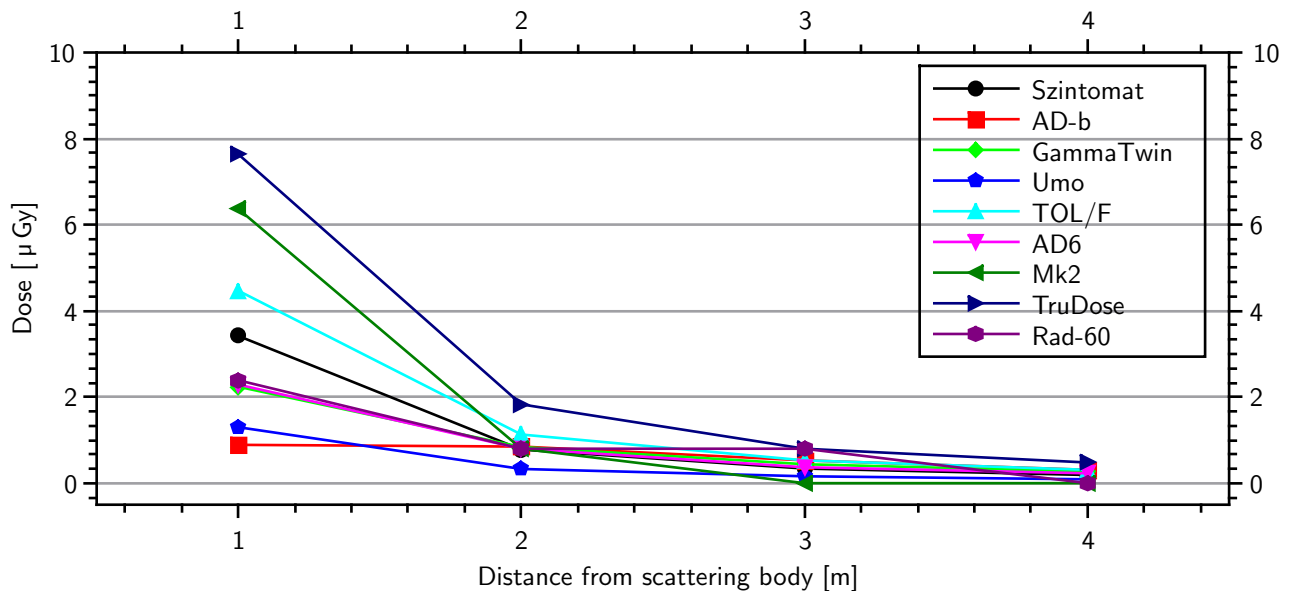


Figure 6.2.8: Dose measurement results of all devices.

Due to a lack of a standard, no statement about the correct functioning of each individual device can be made. A possibility solution for future research would be a simulation in order to estimate the dose rate at all measurement points. However difficulties may arise when trying to adapt the results to devices measuring different variables (e.g.  $H^*(10)$  or  $H_p(10)$ )

## 6.3 Useful radiation

In normal conditions, work is not carried out by the medical personal in the direct unattenuated useful beam. However, in case of an accident, it is important to have a correctly working measuring device. Also for area monitoring it can be necessary to measure in the direct useful radiation. In contrast to the measurements in the stray radiation, the Unfors was not only used to verify constant radiation conditions. Due to the optimisation of the device also for pulsed radiation fields, the measured dose can be used as a standard. The measurements were carried out under the same radiation settings as the measurements in the stray radiation.

The results for the devices of category 1 and 2 are shown in table 6.3.1 the ones for category 3 in table 6.3.2:

Device	Szintomat	AD-b	GammaTwin	Umo	TOL/F	AD6
Voltage [kV]	87.5	87.1	88.5	89.2	88.4	89.5
Meas. time [s]	30	30	29.87	29.87	30	29.87
Dose rate Unfors [ $\mu\text{Gy/s}$ ]	179.0	181.2	179.7	180.7	177.9	181.5
Dose Unfors [ $\mu\text{Gy}$ ]	5356	5420	5364	5382	5308	5442
Dose rate device [mSv/h]	350	0.0999	1.4	14.2	4.2	0.717
Dose device [ $\mu\text{Sv}$ ]	2699	2.3	11.39	111.3	32.19	5.91
Dose device [ $\mu\text{Gy}$ ]	1697	1.45	7.16	97.55	32.19	5.91
Abs. deviation dose [ $\mu\text{Sv}$ ]	-3659	-5419	-5357	-5284	-5280	-5437
Relative deviation dose [%]	-68.31	-99.97	-99.87	-98.19	-99.47	-99.90

Table 6.3.1: Dose measurement results of category 1 and 2 devices in the useful beam.

Device	Mk2	TruDose	Rad-60
Voltage [kV]	88.0	87.8	87.89
Meas. time [s]	29.87	29.87	29.83
Dose Unfors [ $\mu\text{Gy}$ ]	7236		
Dose device [ $\mu\text{Sv}$ ]	2516	18500	2050
Dose device [ $\mu\text{Gy}$ ]	2003	14729	1632
Abs. deviation dose [ $\mu\text{Sv}$ ]	-5233	+7493	-5603
Relative deviation dose [%]	-72.32	+103.56	-77.44

Table 6.3.2: Dose measurement results of category 3 devices in the useful beam.

Because the displayed dose rate of many devices steadily increased during the exposure, no reasonable error could be stated for the dose rates in table 6.3.1.

Since the EPDs were fixed on a scattering body and the Unfors does not measure correct dose values with back scatter radiation, another method had to be found. After the measurement of the EPDs, three measurements of the dose with the Unfors without a scattering body  $D_{\text{Unfors},0 \text{ cm}}$  were taken. With the distance square law the dose on the height of the EPDs  $D_{\text{Unfors},15 \text{ cm}}$  was calculated:

$$D_{\text{Unfors},15 \text{ cm}} = \frac{D_{\text{Unfors},0 \text{ cm}} \cdot 97.5^2}{82.5^2} \quad (6.1)$$

The three results were then averaged and assumed for all EPDs.



The differences in size immediately stand out in the measurement results of the tested devices. Except the TruDose, all devices measure much lower doses than the Unfors, which serves as the standard.

In figure 6.3.1 the absolute dose values of the respective device and Unfors, measured in the useful beam, are illustrated:

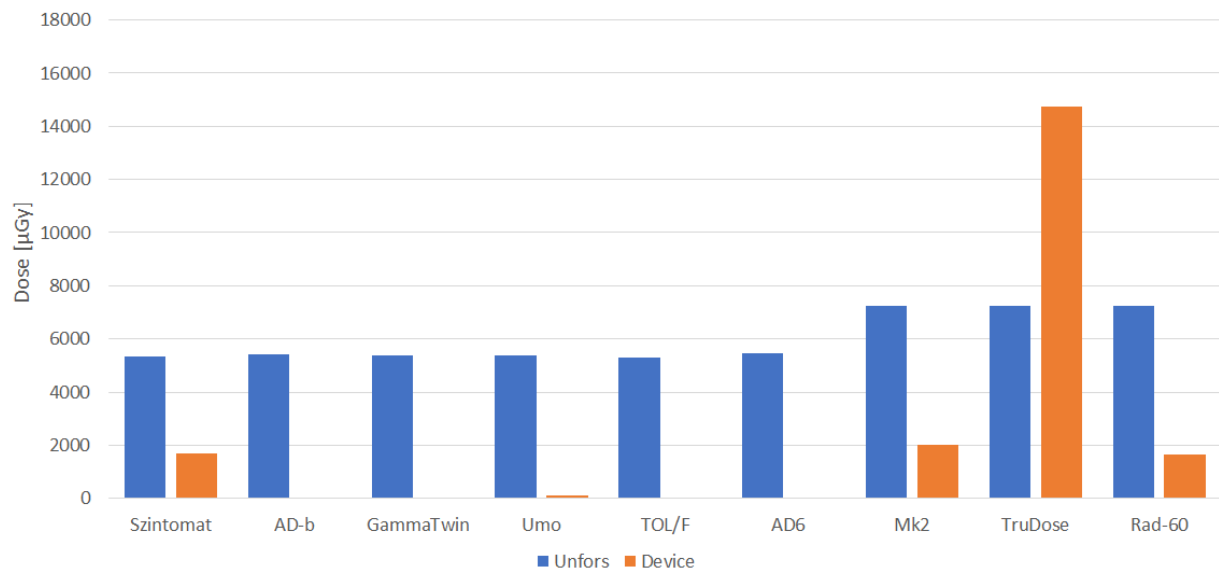


Figure 6.3.1: Absolute dose comparison in the useful radiation.

The y-axis on which the dose is plotted was deliberately scaled linearly in order to point out the tremendous deviations of measured and actual dose.

In figure 6.3.2 the relative deviations between measured and actual dose of the individual measurement devices are plotted:

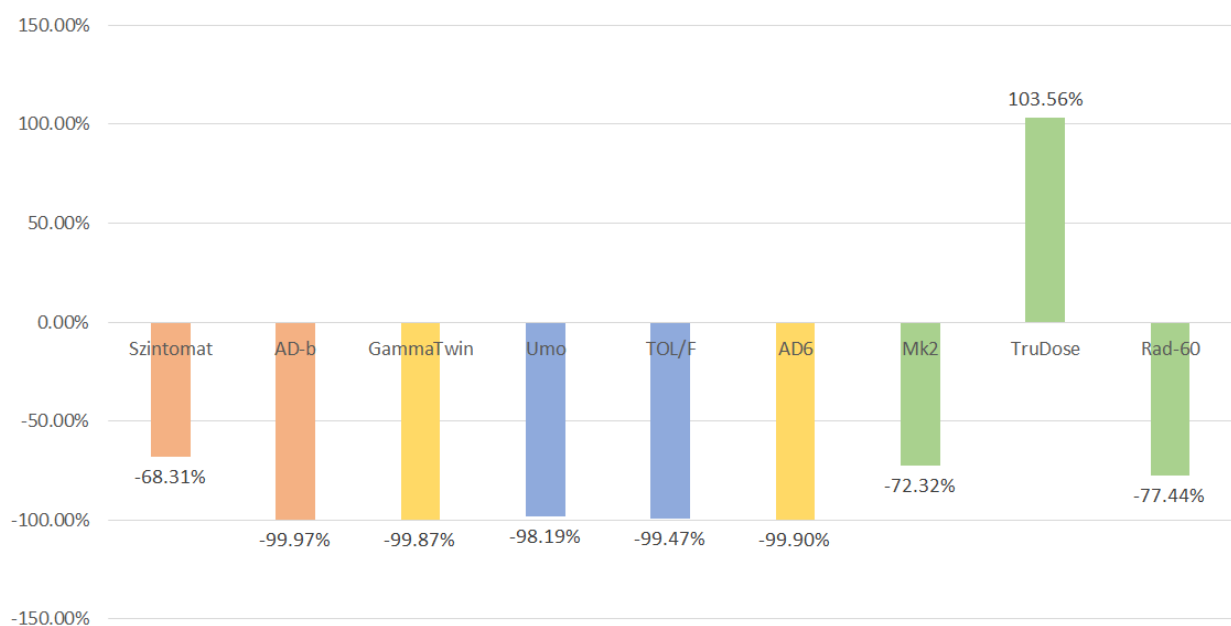


Figure 6.3.2: Absolute dose comparison in the useful radiation.

The specification of the deviation to two decimal places is due to the many approximations and conversions more than actually permissible. However, it allows to clarify the magnitude of deviation and makes different devices comparable.

The colours represent the different detector types. Orange for scintillators, blue for ionisation chambers, yellow for Geiger-Müller counter and green for semi conductors.

While the Szintomat measures at least one third of the dose in the useful beam the AD-b fails completely with only 3/10.000 of the actual dose being detected. However, the maxing out has to be taken into account.

Also, all gas counters fail in the useful beam with a maximum of less than 2% of the dose being detected.

The Mk2 and Rad-60 both detect less than 30% of the dose in the useful beam. The TruDose on the other hand over corrects by displaying more than there actually is. While generally this is in accordance to the conservatism of radiation protection, displaying twice the actual dose is exaggerated. Since, from a purely physical point of view, no more dose can be measured than there is, the value is expected to be over corrected in a calculation.

It must be noted, that the main reason for the deviations presumably is not the pulsation, but the high dose rate. The dose rate in the useful beam is around 0.65 Sv/h, which is much higher than the measuring range of the area monitoring devices.

## 6.4 Recommendations

Based on the results of the measurements carried out the following conclusions can be drawn:

As it turns out, measuring devices for area monitoring seem to work similar in the stray radiation in distance up to 2 m. Closer, the measured dose values start to diverge drastically.

The EPDs on the other hand perform worse in further distances with low dose rate. This, to some part, can be attributed to the integer dose display of the Mk2 and Rad-60.

In the useful beam it is fair to say, that the AD-b, GammaTwin, Umo, TOL/F and AD6 completely fail. Hereby, the measuring range of the devices has to be recognised. The Szintomat, Mk2 and Rad-60 work to some extent with around 30% of the actual dose being measured. Only the TruDose does not measure less than the actual dose, however the display of twice as much still is a big deviation. Nevertheless, in terms of the conservatism of radiation protection, the TruDose is recommended for applications where a dose assessment in a pulsed useful beam could be necessary. Still, the over correction of the device should be kept in mind.

Overall, it could be determined that all devices work best in the areas they were designed for. Devices for area monitoring at some distance in the stray radiation, the EPDs in the useful radiation and close stray radiation.

Main challenges of this thesis were the comparison of devices of different categories and the lack of a standard in the stray radiation. Since conversion factors currently only exist for idealised radiation fields, a comparison of different devices is only possible in approximate terms. However, if in the future new insights are emerging in this field the results of this thesis can be adapted. As already explained in section 6.2.6, a standard for the comparison of displayed and real dose can in principle be achieved with simulations, challenges with the conversion of units may arise.

The results of this thesis confirm that there are serious problems with the detection of pulsed ionising radiation in medical applications with devices that can be officially calibrated in Austria. Due to relevance of the topic for the health of medical professionals further research in this field is highly recommended.

It must be noted, that all conclusions and recommendations are based on the specific settings and components of the experiments. The change of radiation source, for example with different radiation parameter, could have an tremendous effect on the measurement results. One must be aware of this when extrapolating or generalising the findings of this thesis.

# List of Figures

1.2.1	Definition of the impact parameter $s$ with impact centre $Z$ and scattering angle $\varphi$ . [5, p. 248] . . . . .	4
1.2.2	Angular photon distribution for thin absorbers (left) and thick absorbers (right). [5, p. 268] . . . . .	5
1.2.3	Areas representing the dominance of photo effect $\tau$ , Compton effect $\sigma$ and pair production $\kappa$ . The dotted line at $Z = 7$ represents the medium atomic number of human tissue and phantom materials. [5, p. 193] . . . . .	6
1.2.4	Photon energy dependence on the scattering angles. From left to right: 10, 50, 200 keV, 1, 2 and 10 MeV. [5, p. 171] . . . . .	6
1.3.1	Typical sigmoidal curve shape for the relative effect function of deterministic effects. Individual curves vary in terms of dose threshold $S$ , slope, 50%-dose $D_{50}$ , saturation dose $D_{\max}$ and depend both on the irradiated tissue as well as the type of ionising radiation. [5, p. 437] . . . . .	7
1.3.2	Possible relations of dose and radiation damage. [11, p. 91] . . . . .	8
2.1.1	Early application of fluoroscopy. The useful beam is directed on the patient and radiologist who observes the X-ray projection on a fluorescent plate. No precautions for radiological protection were taken. [18, p. 6] . . . . .	12
2.2.1	Frequency of various examination methods using ionising radiation and the share of the collective dose caused by it. [19, p. 8] . . . . .	13
2.4.1	Schematic structure of an X-ray tube. [21, p. 8] . . . . .	15
2.4.2	Typical X-ray spectrum. [22, Production of X-ray] . . . . .	16
2.4.3	Effect on the spectrum by voltage (left), current (middle) and filtration (right). [22, Production of X-ray] . . . . .	16
2.4.4	Radiation fields of the an X-Ray tube. . . . .	17
3.0.1	Schematic plot of the radiation dose of continuous and pulsed fluoroscopy . . . . .	19
3.0.2	Equivalent trapezoidal radiation pulse with the relevant parameters. [27, p. 5] . . . . .	20
4.4.1	Operation modes of an ionisation chamber. [32] . . . . .	24
4.4.2	Function of a scintillation counter. [33] . . . . .	25

5.1.1	C-arm (left) and mobile viewing station (right).	27
5.3.1	RaySafe Unfors Xi	30
5.3.2	RaySafe Unfors X2	30
5.3.3	All examined devices except the Rad-60. Lower row from left to right: AD6 with attached AD-b, Szintomat, Umo, TOL/F. Upper row from left to right: GammaTwin, Mk2, TruDose.	31
5.3.4	Szintomat 6134 A/H	32
5.3.5	6150AD-b/E	32
5.3.6	GammaTwin	33
5.3.7	LB 123 Umo	33
5.3.8	TOL/F LB 1320	34
5.3.9	6150AD6/E	34
5.3.10	EPD Mk2	35
5.3.11	EPD TruDose G	35
5.3.12	Rad-60SE	36
5.4.1	Scattered radiation field of an X-ray tube at 70 kV. [37, p. 4]	37
5.4.2	Experimental setup for stray radiation.	37
5.4.3	Experimental setup for useful radiation.	38
5.4.4	The EPDs and Unfors in the useful beam. From left to right: Mk2, TruDose, Rad-60.	38
6.1.1	Voltage curve large view.	40
6.1.2	Voltage curve detail view.	40
6.2.1	Setup of the measuring devices.	40
6.2.2	Dose measurements results category 1 devices.	42
6.2.3	Dose measurements results category 2 devices.	43
6.2.4	Dose measurements results category 3 devices.	44
6.2.5	Conversion factors between measurement variables. [39, p. 26, 35, 217]	45
6.2.6	Dose measurement results of all devices. Category 1 devices in black, category 2 devices in red, and category 3 devices in green.	46
6.2.7	Dose measurement results of all detector types. Scintillators in black, Geiger-Müller counter in red, ionisation chamber in green and pin diodes in blue.	47
6.2.8	Dose measurement results of all devices.	48
6.3.1	Absolute dose comparison in the useful radiation.	50
6.3.2	Absolute dose comparison in the useful radiation.	50

# List of Tables

5.3.1	Technical data RaySafe Unfors Xi . . . . .	30
5.3.2	Technical data RaySafe Unfors X2 . . . . .	30
5.3.3	Tested devices . . . . .	31
5.3.4	Technical data Szintomat 6134 A/H . . . . .	32
5.3.5	Technical data 6150AD-b/E . . . . .	32
5.3.6	Technical data GammaTwin . . . . .	33
5.3.7	Technical data LB 123 Umo . . . . .	33
5.3.8	Technical data TOL/F LB 1320 . . . . .	34
5.3.9	Technical data 6150AD6/E . . . . .	34
5.3.10	Technical data EPD Mk2 . . . . .	35
5.3.11	Technical data EPD TruDose G . . . . .	35
5.3.12	Technical data Rad-60SE . . . . .	36
6.1.1	Pulse properties at different frame rates. . . . .	39
6.2.1	Voltage, dose rate and radiation time in the useful beam of all measurements in the stray radiation . . . . .	41
6.2.2	Dose measurement results category 1 devices. . . . .	42
6.2.3	Dose measurements results category 2 devices. . . . .	43
6.2.4	Dose measurements results category 3 devices. . . . .	44
6.2.5	Averaged dose measurement results of all categories. . . . .	45
6.2.6	Dose measurement results of all devices in $\mu\text{Gy}$ . . . . .	46
6.2.7	Dose measurement results of all detector types. . . . .	47
6.2.8	Averaged dose measurement results of all devices. . . . .	48
6.3.1	Dose measurement results of category 1 and 2 devices in the useful beam. . . . .	49
6.3.2	Dose measurement results of category 3 devices in the useful beam. . . . .	49

# Bibliography

- [1] Österreichischer Nationalrat. Bundesgesetz über Maßnahmen zum Schutz vor Gefahren durch ionisierende Strahlung (Strahlenschutzgesetz 2020 – StrSchG 2020). Bundesrecht konsolidiert, August 2020.
- [2] International Commission on Radiation Units and Measurements. ICRU Report 33 - Radiation Quantities and Units. *International Commission on Radiation Units and Measurements*, 1980.
- [3] W. Snyder, M. Cook, E. Nasset, L. Karhausen, G. Howells, and I. Tipton. ICRP Publication 23: Report of the Task Group on Reference Man. *International Commission on Radiological Protection*, 1975.
- [4] Lars Persson. On the boundary between ionizing and non-ionizing radiation. *Health Physics*, 1992.
- [5] Hanno Krieger. *Grundlagen der Strahlungsphysik und des Strahlenschutzes - 3. Edition*. Springer-Verlag, 2009.
- [6] Claus Grupen, Tilo Stroh, and Ulrich Werthenbach. *Grundkurs Strahlenschutz: Praxiswissen für den Umgang mit radioaktiven Stoffen*. Springer-Verlag, 2008.
- [7] Energie Mobilität Innovation und Technologie Bundesministerium für Klimaschutz, Umwelt. Radioaktivität und Strahlung in Österreich 2017 bis 2019, 2020.
- [8] International Commission on Radiological Protection. Statement on tissue reactions. *ICRP*, 4825, 2011.
- [9] D. Wolff and K.W. Heinrich. Strahlenschäden der Haut nach Herzkatheterdiagnostik und Therapie. *Hautnah Dermatologie*, 5, 1993.
- [10] International Commission on Radiological Protection. The ICRP 2007 Recommendations. *Radiation Protection Dosimetry*, 127, 2007.
- [11] Wolfgang Schlegel, Christian P. Karger, and Oliver Jäkel. *Medizinische Physik: Grundlagen - Bildgebung - Therapie - Technik*. Springer-Verlag, 2018.
- [12] World Health Organization. *WHO report on cancer: setting priorities, investing wisely and providing care for all*. World Health Organization, 2020.
- [13] Jack Valentin. Low-dose extrapolation of radiation-related cancer risk. *Annals of the ICRP*, 35(4), 2005.
- [14] Public Health England. Medical radiation: uses, dose measurements and safety advice. <https://www.gov.uk/government/collections/medical-radiation-uses-dose-measurements-and-safety-advice>, 2014. Last checked: 17.04.2021.

- [15] E. Posner. Reception of Röntgen's discovery in Britain and U.S.A. *BMJ*, 4, 1970.
- [16] Marcio Luis Ferreira Nascimento. Brief history of X-ray tube patents. *World Patent Information*, 37, 2014.
- [17] Radiologie.de. Entwicklung der Röntgentechnik. <https://www.radiologie.de/entwicklung-der-rontgentechnik/>, 2021. Last checked: 08.03.2021.
- [18] Edwin J. Houston. Elementary Electricity ch. 13: The X-rays. *Popular Electricity magazine*, 2(1), 1908.
- [19] David Wachabauer, Andreas Stoppacher, and Stefan Mathis-Edenhofer. Häufigkeiten medizinischer Anwendungen ionisierender Strahlung in Österreich. Analysen und Empfehlungen auf Basis des Datenjahres 2015. Gesundheit Österreich, 2017.
- [20] Guillermo Avendaño Cervantes. *Technical fundamentals of radiology and CT*. IOP Publishing, University of Valparaiso, Chile, 2016.
- [21] Rita Roque. X-ray imaging using 100 µm thick Gas Electron Multipliers operating in Kr-CO<sub>2</sub> mixtures. PhD thesis, University of Coimbra, Portugal, 2018.
- [22] Sarah Abdulla. Production of X-rays. <https://www.radiologycafe.com/radiology-trainees/frcr-physics-notes/production-of-x-rays>, 2021. Last checked: 11.05.2021.
- [23] Austrian Standards Institute. ÖNORM S 5212 - Medical X-ray equipment up to 300 kV — Radiation protection rules for the installation, 2016.
- [24] Bundesministerin für Gesundheit und Frauen. Verordnung der Bundesministerin für Gesundheit und Frauen über Maßnahmen zum Schutz von Personen vor Schäden durch Anwendung ionisierender Strahlung im Bereich der Medizin (Medizinische Strahlenschutzverordnung – MedStrSchV). Bundesrecht konsolidiert, 2017.
- [25] Peter Ambrosi, Markus Borowski, and Michael Iwatschenko. Considerations concerning the use of counting active personal dosimeters in pulsed fields of ionising radiation. *Radiation Protection Dosimetry*, 139(4), 2010.
- [26] Andreas Steurer; Hannes Stadtmann; Alfred Hefner. Dosis- und Dosisleistungsmessungen bei gepulster Strahlung - Reagieren die eingesetzten Messgeräte richtig? ARC Seibersdorf Research GmbH, A-2444 Seibersdorf, 2003.
- [27] International Organization for Standardization. Radiological protection — Characteristics of reference pulsed radiation — Part 1: Photon radiation, 2015.
- [28] Wikipedia. Kerma. <https://en.wikipedia.org/wiki/Kerma>. Last checked: 17.04.2021.
- [29] P. Ambrosi. Messtechnische Probleme elektronischer Dosimeter in gepulsten Strahlungsfeldern. In *13. Fortbildungsseminar der APT*. Physikalisch-Technische Bundesanstalt, 2009.
- [30] E. M. I. und T.; Bundesminister für Soziales G. P. und K. und Bundesministerin für Digitalisierung und W. Bundesministerin für Klimaschutz, U. Allgemeine Maßnahmen zum Schutz vor Gefahren durch ionisierende Strahlung (Allgemeine Strahlenschutzverordnung 2020 – AllgStrSchV 2020). Bundesrecht konsolidiert, 2020.
- [31] Österreichischer Nationalrat. Bundesgesetz vom 5. Juli 1950 über das Maß- und Eichwesen (Maß- und Eichgesetz - MEG). Bundesrecht konsolidiert, 1950.
- [32] Wikipedia. Practical Gaseous Ionisation Detection Regions. <https://en.wikipedia.org/wiki/Ionization-chamber>, 2021. Last checked: 17.04.2021.



- [33] Wikipedia. Scintillation counter. <https://en.wikipedia.org/wiki/Scintillation-counter>, 2021. Last checked: 17.04.2021.
- [34] Oliver Hupe, Hayo Zutz, and Jana Klammer. Radiation protection dosimetry in pulsed radiation fields. Physikalisch-Technische Bundesanstalt (PTB), 2012.
- [35] Frank Busch. Gepulste Röntgenstrahlung - Welche Messgeräte wären einsetzbar?! - Stand und Entwicklung. 16. Seminar Aktuelle Fragen der Durchstrahlungsprüfung und des Strahlenschutzes – Vortrag 7, 2014.
- [36] Philips Medical Systems. *BV Pulsera Manual*, 2.1 edition.
- [37] Hanno Krieger. Praktischer Strahlenschutz im Röntgen. Springer-Verlag, 2015.
- [38] Hamish Smith; Monica Wong. X-ray quantity and quality. <https://radiopaedia.org/articles/x-ray-quantity-and-quality>. Last checked: 18.04.2021.
- [39] Strahlenschutzkommission. Berechnungsgrundlage für die Ermittlung von Körper-Äquivalentdosen bei äußerer Strahlenexposition. Bundesministerium für Umwelt, Naturschutz, Bau und Reaktorsicherheit, 2017.

# Glossary

**Radiosensitivity** - Susceptibility of cells to the effects of ionising radiation.

**Cell differentiation** - Measure for the specialisation of cells. The more specific the task of a cell, the harder it is to replace.

**Life span study** - Epidemiological study investigating long-term health effects of A-bomb survivors of Hiroshima and Nagasaki.

**Radiation erythema** - Tissue reaction characterised by reddening of the skin due to too high a radiation dose. Can have a latency period of several weeks which can severely complicate the cause identification.

**Acute radiation syndrome** - Acute illness due to extensive exposition to a high dose of ionising radiation within a short time span. Typical symptoms include nausea, headache, vomiting and fever. Also known as radiation sickness or radiation poisoning.

**Necrosis** - Contrary to the apoptosis, the orderly mortification of a single or multiple cells, necrosis describes the uncontrolled death due to an external influence. Often associated with an inflammatory reaction.

**Somatic effects** - Effects limited to the individual in contrast to for example heritable genetic defects.

**Haemogram** - Group of tests performed on a blood sample. Also known as blood count.

**Linear no threshold** - Model in radiation protection according to which there is a linear relation between dose and stochastic effects with even small doses being harmful. It corresponds to the conservative safety first approach of radiation protection.

**Relative biological effectiveness** - Factor used in radiobiology to evaluate different types of ionising radiation in terms of their harmfulness to biological systems.

**Interventional radiology** - Minimally invasive surgical procedures using medical imaging with ionising radiation for guidance.

**Exploratory surgery** - Surgical intervention used for diagnosis, not treatment. Due to modern imaging techniques exploratory surgery in humans has become very rare.

**Sectional imaging techniques** - Number of advanced imaging techniques that enable to image the body in cross section (e.g. CT or MRT)

**Latency period** - Time span between exposure to a stimulation and a bodily reaction to it.

**DNA double strand breaks** - A damage in both strands of the double helix is especially dangerous, because DNA repair mechanisms can only be applied to a limited extend.

**Radicals** - Highly reactive chemical compound with unpaired electrons. Can rip electrons from other molecules and impair the DNA.

**Vascular examination** - Examination of vessels, often with the use of a contrast medium to enhance the density gradient.

**Half value layer thickness** - Thickness of a material after the passage of which the radiation intensity has decreased by half. However, the overproportional absorption of low energy photons must be kept in mind. This causes, that after two half value layer thicknesses the intensity is not reduced to  $1/4$  but a little less.